

# Metadata of the article that will be visualized in OnlineFirst

|                      |  |   |
|----------------------|--|---|
| ArticleTitle         | Back to black: a mineralogical and chemical characterisation of Atticising fourth century BCE black gloss ware |   |
| Article Sub-Title    |  |   |
| Article CopyRight    | The Author(s)<br>(This will be the copyright line in the final PDF)  |   |
| Journal Name         | Archaeological and Anthropological Sciences  |   |
| Corresponding Author | FamilyName   | <b>Solard</b>   |
|                      | Particle   |   |
|                      | Given Name   | <b>Baptiste</b>   |
|                      | Suffix   |   |
|                      | Division   | Archaeometry research group, Competence Center Archaeometry – Baden-Wuerttemberg        |
|                      | Organization   | Universität Tübingen  |
|                      | Address  | Tübingen, Germany   |
|                      | Phone  |   |
|                      | Fax  |   |
|                      | Email  | baptiste.solard@gmail.com   |
|                      | ORCID  | <a href="http://orcid.org/0000-0002-8215-5721">http://orcid.org/0000-0002-8215-5721</a> |
| Author               | FamilyName   | <b>Amicone</b>  |
|                      | Particle   |   |
|                      | Given Name   | <b>Silvia</b>   |
|                      | Suffix   |   |
|                      | Division   | Archaeometry research group, Competence Center Archaeometry – Baden-Wuerttemberg        |
|                      | Organization   | Universität Tübingen  |
|                      | Address  | Tübingen, Germany   |
|                      | Division   | Institute of Archaeology  |
|                      | Organization   | University College London   |
|                      | Address  | London, UK  |
|                      | Phone  |   |
|                      | Fax  |   |
|                      | Email  |   |
|                      | ORCID  | <a href="http://orcid.org/0000-0001-8237-7044">http://orcid.org/0000-0001-8237-7044</a> |
| Author               | FamilyName   | <b>Aloupi-Siotis</b>  |
|                      | Particle   |   |
|                      | Given Name   | <b>Eleni</b>  |
|                      | Suffix   |   |
|                      | Division   |   |
|                      | Organization   | THETIS AUTHENTICS LTD   |
|                      | Address  | Athens, Greece  |
|                      | Phone  |   |
|                      | Fax  |   |
|                      | Email  |   |
|                      | ORCID  | <a href="http://orcid.org/0000-0003-4957-3777">http://orcid.org/0000-0003-4957-3777</a> |
|                      | URL  |   |

|          |  |   |
|----------|--|---|
| Author   | FamilyName   | <b>Heinze</b>   |
|          | Particle   |   |
|          | Given Name   | <b>Lars</b>   |
|          | Suffix   |   |
|          | Division   | Archäologisches Institut  |
|          | Organization   | Universität zu Köln   |
|          | Address  | Cologne, Germany  |
|          | Phone  |   |
|          | Fax  |   |
|          | Email  |   |
|          | URL  |   |
|          | ORCID  | <a href="http://orcid.org/0000-0002-0899-6688">http://orcid.org/0000-0002-0899-6688</a> |
| Author   | FamilyName   | <b>Berti</b>  |
|          | Particle   |   |
|          | Given Name   | <b>Fede</b>   |
|          | Suffix   |   |
|          | Division   |   |
|          | Organization   | The Italian Archaeological Mission of Iasos   |
|          | Address  | Milas, Turkey   |
|          | Phone  |   |
|          | Fax  |   |
|          | Email  |   |
|          | URL  |   |
|          | ORCID  |   |
| Author   | FamilyName   | <b>Lambrugo</b>   |
|          | Particle   |   |
|          | Given Name   | <b>Claudia</b>  |
|          | Suffix   |   |
|          | Division   | Dipartimento di Beni Culturali e Ambientali   |
|          | Organization   | Università degli Studi di Milano  |
|          | Address  | Milan, Italy  |
|          | Phone  |   |
|          | Fax  |   |
|          | Email  |   |
|          | URL  |   |
|          | ORCID  |   |
| Author   | FamilyName   | <b>Berthold</b>   |
|          | Particle   |   |
|          | Given Name   | <b>Christoph</b>  |
|          | Suffix   |   |
|          | Division   | Archaeometry research group, Competence Center Archaeometry – Baden-Wuerttemberg        |
|          | Organization   | Universität Tübingen  |
|          | Address  | Tübingen, Germany   |
|          | Phone  |   |
|          | Fax  |   |
|          | Email  |   |
|          | URL  |   |
|          | ORCID  |   |
| Schedule | Received   | 14 Mar 2023   |
|          | Revised  |   |
|          | Accepted   | 4 Jul 2023  |
| Abstract | Most previous studies on Attic black gloss technology focused on productions from Greece, especially Athens. However, the black gloss technique constitutes the most widespread decoration practice across |   |

the Mediterranean from the Archaic to the Hellenistic periods. Focusing on both Attic and Atticising black gloss productions from sites in Sicily and Asia Minor, our work aims to shed new light on the technology of this decoration and its transmission throughout the Mediterranean during the fourth century BCE. Additionally, to investigate the technological relationship between black and the less common intentional red gloss decorations, a selection of bichrome black-and-red and red gloss vessels were included in this study. For this purpose, we applied an integrated analytical approach, aiming to characterise both the chemistry and the mineralogy of archaeological black and red gloss decorations. This approach includes ceramic petrography, pXRF,  $\mu$ -XRD2, and SEM-EDS. Specimens from the fourth century BCE from Manfria (*chora* of Gela), Iasos (Caria), and Priene (Ionia) were analysed. These assemblages reflect various production groups identified by the chemical and petrographic analyses of the ceramic bodies. The  $\mu$ -XRD2 and SEM-EDS measurements of the gloss show a certain degree of mineralogical and chemical variability that does not necessarily correlate with the recognised production groups but, rather, reflects different technological practices. Despite this variability, the results suggest that the various gloss productions were produced with a very similar technological process and offer new insights into the mechanisms through which the black gloss technique diffused throughout the Mediterranean.

---

|                             |   |
|-----------------------------|---|
| Keywords (separated by '-') | Atticising black gloss - Pyrotechnology - Clay raw material - Technological transmission - Archaeometry |
|-----------------------------|---|

---

|                      |   |
|----------------------|---|
| Footnote Information | The online version contains supplementary material available at <a href="https://doi.org/10.1007/s12520-023-01822-4">https://doi.org/10.1007/s12520-023-01822-4</a> . |
|----------------------|---|

---



## RESEARCH

# Back to black: a mineralogical and chemical characterisation of Atticising fourth century BCE black gloss ware

Baptiste Solard<sup>1</sup> · Silvia Amicone<sup>1,2</sup> · Eleni Aloupi-Siotis<sup>3</sup> · Lars Heinze<sup>4</sup> · Fede Berti<sup>5</sup> · Claudia Lambrugo<sup>6</sup> · Christoph Berthold<sup>1</sup>

Received: 14 March 2023 / Accepted: 4 July 2023  
 © The Author(s) 2023

## Abstract

Most previous studies on Attic black gloss technology focused on productions from Greece, especially Athens. However, the black gloss technique constitutes the most widespread decoration practice across the Mediterranean from the Archaic to the Hellenistic periods. Focusing on both Attic and Atticising black gloss productions from sites in Sicily and Asia Minor, our work aims to shed new light on the technology of this decoration and its transmission throughout the Mediterranean during the fourth century BCE. Additionally, to investigate the technological relationship between black and the less common intentional red gloss decorations, a selection of bichrome black-and-red and red gloss vessels were included in this study. For this purpose, we applied an integrated analytical approach, aiming to characterise both the chemistry and the mineralogy of archaeological black and red gloss decorations. This approach includes ceramic petrography, pXRF,  $\mu$ -XRD<sup>2</sup>, and SEM-EDS. Specimens from the fourth century BCE from Manfria (*chora* of Gela), Iasos (Caria), and Priene (Ionia) were analysed. These assemblages reflect various production groups identified by the chemical and petrographic analyses of the ceramic bodies. The  $\mu$ -XRD<sup>2</sup> and SEM-EDS measurements of the gloss show a certain degree of mineralogical and chemical variability that does not necessarily correlate with the recognised production groups but, rather, reflects different technological practices. Despite this variability, the results suggest that the various gloss productions were produced with a very similar technological process and offer new insights into the mechanisms through which the black gloss technique diffused throughout the Mediterranean.

**Keywords** Atticising black gloss · Pyrotechnology · Clay raw material · Technological transmission · Archaeometry

## Introduction

Ceramic decoration techniques, the external display of a potter's skills and technical knowledge, are a major focal point for archaeological studies aiming to understand ancient potters' mastery of raw material processing and pyrotechnology as well as the mechanisms by which this know-how was transmitted through space and time. Black gloss<sup>1</sup> decoration, one of the most characteristic techniques of the Classical period, has been the object of many archaeometric analyses (Aloupi-Siotis 2020).

The black gloss technique was first introduced around 700 BCE in Corinth (Boardman 1974, p. 9; Jones 2021), reaching its technological and aesthetic peak between the

✉ Baptiste Solard  
 baptiste.solard@gmail.com

<sup>1</sup> Archaeometry research group, Competence Center Archaeometry – Baden-Wuerttemberg, Universität Tübingen, Tübingen, Germany

<sup>2</sup> Institute of Archaeology, University College London, London, UK

<sup>3</sup> THETIS AUTHENTICS LTD, Athens, Greece

<sup>4</sup> Archäologisches Institut, Universität zu Köln, Cologne, Germany

<sup>5</sup> The Italian Archaeological Mission of Iasos, Milas, Turkey

<sup>6</sup> Dipartimento di Beni Culturali e Ambientali, Università degli Studi di Milano, Milan, Italy

<sup>1</sup> In recent years, the use of the term “gloss” for black gloss has been debated (see Aloupi-Siotis 2020, pp. 7–8; Jones 2021; and literature therein). However, to ensure terminological continuity with previous research on the studied materials, the term “gloss” is used here.

sixth and the fourth centuries BCE with the Attic black gloss vessels produced in Attica (Aloupi-Siotis 2020; Chaviara 2014; Lühl et al. 2014; Tang et al. 2001; Walton et al. 2004). These vessels flooded the Mediterranean pottery market and, consequently, new productions started in other regions (Giorgetti et al. 2004; Maggetti et al. 1981; Mirti 1996; Mirti and Davit 2008; Vendrell-Saz et al. 1991). These local reproductions, referred to today as Atticising black gloss, are key to understanding the transmission of technological know-how between Attic artisans and potters producing Atticising vessels.

The archaeometric study of Attic black gloss started as early as 1752 with the works of Comte de Caylus, who first identified the raw material used for their production as ‘ferruginous earth’. Many further investigations and reproduction experiments in the nineteenth, twentieth, and early twenty-first centuries led to our modern understanding of Attic black gloss technology as a ceramic coating produced from a levigated, non-calcareous, iron- and illite-rich clay slip that has been vitrified through a three-stage oxidising-reducing-oxidising firing (e.g. Bimson 1956; Binns and Fraser 1929; Chaviara and Aloupi-Siotis 2016; Gliozzo et al. 2004; Lühl et al. 2014; Maniatis et al. 1993; Noble 1960; Tite et al. 1982; Winter 1978). However, few archaeometric works have investigated the production techniques of Atticising black gloss (e.g. Amicone 2015; Gliozzo et al. 2004; Mirti et al. 1996), thus leaving the question of the transmission of technological knowledge from Attica throughout the Mediterranean as of yet largely unanswered.

The primary aim of this work is to better understand the production of the black gloss technique, especially regarding the transmission of know-how between Attic potters and the manufacturers of Atticising vessels during the fourth century BCE, a period in which the Atticising black gloss productions flourished around the Mediterranean. Additionally, the secondary goal of this study is to expand our knowledge of the technological relationship between the production techniques of black and contemporary red iron-based gloss decorations. To address these goals, assemblages containing Attic and Atticising gloss ware from Manfria (Sicily), as well as Iasos and Priene (both Asia Minor), are characterised using an integrated approach combining petrographic, elemental, and mineralogical analyses. The gloss ware assemblages from these three sites were selected for this study as they provide a view of the different black gloss productions in the Mediterranean during the fourth century BCE. The vessels from Iasos and Priene represent the Attic and Eastern Atticising productions, which also encompass bichrome black-and-red and intentional red gloss ware, while those of Manfria serve as an example of the Western Atticising productions.

## Previous studies of Attic gloss technology

It is well known that black gloss was obtained through the application of clay paint on leather-hard vessels before firing. Through combined physicochemical analysis and replication of the process, it is clear that the clay slip was prepared from a fine colloidal suspension of iron-rich, non-calcareous clays with substantial illitic content (Aloupi-Siotis 2008, 2020; Chaviara 2014; Chaviara and Aloupi-Siotis 2016; Giorgetti et al. 2004; Gliozzo et al. 2004; Lühl et al. 2014; Maniatis et al. 1993; Noll et al. 1975; Tite et al. 1982; Walton et al. 2014). The clay slip was produced through levigation of the raw clay (Walton et al. 2014; Winter 1978) or suspension in water (Aloupi-Siotis 2008) followed by peptization and precipitation (Winter 1978). The finest clay fraction was finally thickened via evaporation to produce a concentrated clay paint. The use of raw clays rich in illitic clay minerals is explained by their chemical and mineralogical composition (rich in potassium) and their ability to spontaneously disperse in water without the need for any deflocculating or dispersing agent (Chaviara 2014; Chaviara and Aloupi-Siotis 2016). However, additives such as bone powder, wood, plant, or seaweed ashes could have been used to enhance the dispersion of the clay particles in water (Aloupi-Siotis 2020; Hofmann 1962; Mirti et al. 1996; Noble 1960; Winter 1978).

Clay sources have been investigated to identify the possible raw material zones of supply in Attica. Until now, five sources have presented suitable characteristics to produce black gloss around Athens (Chaviara 2014; Chaviara and Aloupi-Siotis 2016). Nevertheless, similar suitable clay deposits can also be found around the Mediterranean (see Aloupi-Siotis 2020 and literature therein), which could explain the transmission of the black gloss production technique across the region.

Many studies identified the firing scheme of Attic black gloss as a three-stage oxidising-reducing-oxidising process in an updraft kiln (Aloupi-Siotis 2008, 2020; Balachandran 2019; Bente et al. 2013; Binns and Fraser 1929; Chaviara 2014; Cianchetta et al. 2015; Giorgetti et al. 2004; Gliozzo et al. 2004; Jones 2021; Lühl et al. 2014; Madrid i Fernández and Sinner 2019; Noble 1960; Tang et al. 2001; Tite et al. 1982). The first, oxidising stage of the firing, from ambient to maximum temperature (around 850–900°C), consists of thoroughly drying the vessels, dehydration of the clay minerals, sintering, and initiation of vitrification in both the clay body and the paint layer. During the second, reducing stage, the temperature decreases while the iron oxides present in the clay paint and the ceramic body are reduced to iron spinels, magnetite (FeO·Fe<sub>2</sub>O<sub>3</sub>), and hercynite (FeO·Al<sub>2</sub>O<sub>3</sub>), which are responsible for the black colour. Additionally, the reducing conditions accelerate the vitrification of the paint layer and make it impermeable to oxygen, thus sealing the black iron oxides for the rest of the firing. The last,

**Table 1** Mean chemical composition of ancient Attic black gloss sherds (from Aloupi-Siotis 2008)

| Major oxides | Na <sub>2</sub> O | MgO | Al <sub>2</sub> O <sub>3</sub> | SiO <sub>2</sub> | P <sub>2</sub> O <sub>5</sub> | K <sub>2</sub> O | CaO | TiO <sub>2</sub> | MnO | FeO  |
|--------------|-------------------|-----|--------------------------------|------------------|-------------------------------|------------------|-----|------------------|-----|------|
| Content (%)  | 0.7               | 1.9 | 30.0                           | 46.2             | 0.3                           | 5.4              | 0.8 | 0.6              | 0.1 | 14.5 |

reoxidising stage allows for the reoxidation of the ceramic body into the reddish hematite ( $\alpha$ -Fe<sub>2</sub>O<sub>3</sub>). Moreover, this process sees the formation of the brownish reverse spinel maghemite ( $\gamma$ -Fe<sub>2</sub>O<sub>3</sub>) as a transition state iron oxide. Both these iron oxide phases can also be observed in the gloss, depending on how well it was vitrified during the previous stage. It appears that the firing scheme is quite complex and requires a high degree of control over the different parameters, especially because of the very narrow range of temperatures at which the vessels must be fired to produce a good quality black gloss decoration.

On a chemical level, Attic black gloss is typically composed of high amounts of silica, alumina, and iron oxide, with a low CaO content (Table 1) (Jones 2021; Lühl et al. 2014; Maggetti et al. 1981; Scarpelli et al. 2014; Tite et al. 1982; Walton et al. 2014). In terms of mineralogical composition, Attic and Campanian black gloss are composed of hercynite, magnetite, and maghemite, usually associated with quartz and feldspars, and with the occasional presence of hematite (Bente et al. 2013; Berthold et al. 2017; Cianchetta et al. 2015; Gliozzo and Memmi Turbanti 2004; Jones 2021; Lühl et al. 2014; Maggetti et al. 1981; Maniatis et al. 1983; Scarpelli et al. 2014; Tite et al. 1982; Vendrell-Saz et al. 1991; Walton et al. 2014). Moreover, the close dependence of the mineralogical content on the firing conditions again stresses the importance of a high degree of control to produce good-quality black gloss decoration (Cianchetta et al. 2016; Scarpelli et al. 2014).

Several colour effects can be seen between different examples of black gloss. For instance, Gliozzo et al. (2004) and Giorgetti et al. (2004) discriminated seven surface appearance categories in Etruscan black gloss, which depend on the mineralogical content of the gloss. Another study suggested that the high quality of the Attic black gloss is due to the presence of Fe(II) in the spinel nanocrystals dispersed in the gloss, while a greenish hue could appear when the ratio of spinel is higher, and/or due to the presence of Fe(III) (Aloupi-Siotis 2008).

Alongside the black gloss decorations, intentional red gloss can also be observed on Archaic and Classical Greek vessels (Cohen 2006). These red gloss layers were produced from a similar iron-rich clay paint as the black layers but fired in oxidising conditions to produce the hematite red colouration (Binns and Fraser 1929; Maish et al. 2006; Richter 1951; Tite et al. 1982; Walton et al. 2009). The technological challenge represented by intentional red gloss production lies in the coexistence of both black and red gloss coatings in

some vessels. Different hypotheses were suggested to reconstruct the firing of bichrome vessels (Aloupi-Siotis 2008; Farnsworth and Wisely 1958; Richter 1951; Tite et al. 1982; Winter 1978), which involved the use of different clay slips, different clay fractions, or a second firing under oxidising conditions for the production of the red gloss. However, a consensus on this question has not yet been reached.

Overall, the previous archaeometric studies of black gloss vases showed that the pyrotechnological process of their production was far from easy. Therefore, the most plausible explanation for the wide spreading of this sophisticated technique is that the reproduction of black gloss decoration can only be successful when directly transmitted from one experienced potter to another.

## Materials and methods

### Materials

#### Manfria

The *fattoria officina* of Manfria (DMS coordinates: 37° 06' 29" N, 14° 09' 51" E), or Manfria Farm, is a rural site located in the *chora* of Gela (southern Sicily, Italy), approximately 12km west of the city. Gela is a Greek colony founded at the beginning of the seventh century BCE. Archaeological research indicates that habitation at Manfria peaked from the middle of the fifth century BCE to the first half of the fourth century BCE and was generally abandoned in the middle of the fourth century BCE (Lambrugo et al. 2019). A recent re-examination of the pottery assemblage refuted the original interpretation of the site as a rural farm associated with a workshop (Adamesteanu 1958) and proposed a new interpretation as a sanctuary (Amicone 2016). A great number of well-preserved black gloss vessels were recovered from the site, the shapes of which clearly indicate Atticising productions, dating to the second half of the fifth and the first half of the fourth century BCE (Lambrugo et al. 2019). Therefore, this assemblage represents well this type of ware in Gela and its *chora*.

A total of 15 vessels were sampled from the black gloss assemblage of Manfria (Table 2). This sampling was done to represent the diversity in petrographic fabric (see the 'Manfria' section) and vessel shapes of the complete assemblage.

**Table 2** List of the samples with the surface appearance of their black and red gloss respectively

| Site    | Sample no. | Black gloss     | Red gloss     |
|---------|------------|-----------------|---------------|
| Manfria | M1*        | Matt            |               |
|         | M11*       | Metallic        |               |
|         | M17*       | Matt            |               |
|         | M18        | Shiny           |               |
|         | M19        | Matt            |               |
|         | M20        | Matt            |               |
|         | M22        | Matt            |               |
|         | M26*       | Shiny           |               |
|         | M29        | Shiny           |               |
|         | M31        | Shiny           |               |
|         | M33*       | Metallic        |               |
|         | M34        | Metallic        |               |
|         | M40        | Matt            |               |
|         | M42*       | Matt            |               |
|         | M51        | Irregular black |               |
| Iasos   | IA1*       | Shiny           | Red           |
|         | IA2        |                 | Red           |
|         | IA3        | Metallic        |               |
|         | IA4*       | Shiny           |               |
|         | IA5        | Irregular black | Red           |
|         | IA6*       | Shiny           | Red           |
|         | IA7        | Irregular black |               |
|         | IA8        | Matt            |               |
|         | IA9        | Shiny           | Red           |
|         | IA10*      | Matt            | Red           |
| Priene  | IA11       | Shiny           |               |
|         | IA12       | Matt            |               |
|         | IA13*      | Matt            |               |
|         | IA14       | Irregular black | Red           |
|         | IA15       | Shiny           | Red           |
|         | Pri530*    | Shiny           |               |
|         | Pri533*    | Matt greenish   |               |
|         | Pri534     | Shiny           |               |
|         | Pri536*    | Irregular black |               |
|         | Pri540*    | Irregular black |               |
|         | Pri544*    | Irregular black |               |
|         | Pri545     | Irregular black |               |
|         | Pri546     | Irregular black |               |
|         | Pri552     |                 | Red           |
|         | Pri558*    |                 | Red           |
|         | Pri559     |                 | Irregular red |
|         | Pri561     | Matt            |               |
|         | Pri562*    | Matt            |               |
|         | Pri571*    |                 | Red           |
|         | Pri602*    | Matt            |               |
|         | Pri609     | Shiny           |               |
|         | Pri674     | Matt            |               |

\*Sample analysed via SEM-EDS

## Iasos

The ancient Greek city of Iasos (DMS coordinates: 37° 16' 46" N, 27° 35' 03" E) is located in Caria, close to the modern village of Kiyıkışlacık (Muğla Province, Turkey). Black gloss vessels from the fourth century BCE were found in all of the currently excavated parts of the city, both residential and public (Berti 2013). A particularity of the black gloss ware recovered in Iasos is the presence of intentional red gloss associated with the usual black gloss. This is especially common on plates, bolsal cups, and kantharoi. These black and red vessels represent the typical regional production of Atticising vessels in Iasos (Berti 2013) and occasionally occur in Northern Ionia from the end of the fifth century BCE (Cook 1965).

A total of 15 vessels were chosen to represent the productions found in Iasos based on a first macro-fabric description of the complete Iasos assemblage (Table 2). Thirteen of the sherds were dated to the fourth century BCE, while the two others were clearly identified as fifth century BCE Attic black gloss and were thus used as comparative references (Amicone 2015).

## Priene

The ancient Greek city of Priene (DMS coordinates: 37° 39' 32" N, 27° 17' 53" E) is located in Ionia, near the modern village of Güllübahçe (Aydın Province, Turkey). The current location of Priene corresponds to a relocation of the entire city during the middle of the fourth century BCE (Raack 2020, pp. 2-4; Rumscheid 1998, p. 15). In 1998, the University of Frankfurt started new excavations focusing on various residential and public areas of the city. Large amounts of Attic and Atticising vessels were thereby recovered, mainly dating to the fourth and beginning of the third century BCE (Heinze 2014).

Their study (Heinze 2023) led to the identification of 8 distinctive macro-fabrics, supported by chemical data obtained via pXRF. In particular, one macro-fabric represented the Attic black gloss imports in the city of Priene.

Based on this previous study, 17 vessels were selected to best represent the various macro-fabrics and shapes of the gloss ware assemblage (Table 2).

## Surface appearance criteria

Each of the 47 gloss samples' surface appearance was visually assessed and divided into different categories. The black gloss specimens were separated into shiny, metallic, matt, and irregular (Table 2). Black gloss specimens that reflected light with a shiny appearance were characterised as 'shiny' (see 'shining black' and 'vitreous black' in Gliozzo et al. 2004), while the specimens that reflected light with a metallic



appearance were labelled as ‘metallic’. The specimens, which did not reflect light were characterised as ‘matt’. Finally, the black gloss specimens with both black and brownish to reddish areas were labelled as ‘irregular black’.

The red gloss specimens were considered one single surface appearance and were labelled ‘red’, except for Pri559, which was characterised as ‘irregular red’, as it presents both red and brownish areas (Table 2).

## Methods

### Ceramic petrography and portable X-ray fluorescence

To complete the previous ceramic body characterisations of the studied material (Amicone 2015; Heinze 2023), a ceramic petrographic analysis of the Manfria and Priene assemblages was performed alongside a chemical investigation of the Manfria assemblage via pXRF.

For the ceramic petrographic study, each sample was vertically cut in a cross-section, glued to a glass slide, and prepared into a thin section by polishing the sample to a thickness of approximately 30 µm. The examination of the resulting thin sections was done with a petrographic microscope, following Quinn’s guidelines (Quinn 2013, pp. 80–120) to identify the different petrographic fabrics represented in the assemblages.

The chemical characterisation of the ceramic bodies of the Manfria assemblage was performed with a Thermo Scientific Niton XL3t. A detailed description of the instrument can be found in Helfert et al. (2011). Three points across the ceramic body were measured to reinforce the representativity of the measurements and compensate inhomogeneity of the sample. The measurements for each sample were averaged and the major and minor elements, recorded in oxide weight percentage, were normalised to 100% and calculated with respect to the stoichiometry (Helfert 2013, pp. 39–40, Quinn 2022, pp. 358–365). Trace elements were quantified in parts per million. After normalisation, the data were used as such for visual display in bivariate plots. Additionally, a principal component analysis (PCA) was performed using the computer-based statistical package R to create a multivariate scatterplot of the chemical data. This chemical characterisation was carried out following the same methodology, in which the assemblages of Iasos and Priene were studied, to ensure comparability (Amicone 2015; Heinze and 2023).

### Micro-X-ray diffractometry

The mineral composition of the gloss in each sherd was investigated by micro-X-ray diffraction coupled with a two-dimensional detector ( $\mu$ -XRD<sup>2</sup>). This technique permits a high-resolution, local analysis of a sample’s surface with a

small sample volume and does not require any preparation of the sample (Berthold et al. 2009; Berthold and Mentzer 2017) and has already been proven a highly effective analytical technique of Attic black gloss (Berthold et al. 2017). By acquiring the characteristic mineralogical phases present in the gloss, it is possible to obtain information on pyrotechnology, i.e. the firing temperatures and atmospheres of the firing process.

The measurements were carried out with a BRUKER D8 Discover  $\Theta/\Theta$  GADDS micro-diffractometer. The instrument is equipped with a Co-sealed tube, running at 30 kV/30 mA, a HOPG-primary monochromator, and a 500-µm monocapillary optic with a 300-µm pinhole at the exit, producing a beam diameter of 300 µm. The detection system uses a VANTEC-500 2-dimensional detector that covers about 40° in the 2 $\theta$ - and  $\psi$ -range. The usual measurement setup involves a fixed incident beam angle of 10° and two positions for the detector (15 and 40°) with a 4-min measurement time by position. The final diffractogram covers approximately a 60° 2 $\theta$  angle range. The mineral phase identification was performed using the Powder Diffraction File database, available from the International Centre for Diffraction Data (Newtown Square, PA, USA). To guarantee a proper comparison between the measurements, each diffractogram was calibrated on the X-axis with the help of the quartz reflection at 31° 2 $\theta$  (see Supplementary Materials).

For each sample, a total of three individual measurements were taken on the gloss’ surface to obtain the most representative mineralogical composition of the sherd. Additionally, measurements were performed on the surface of a fresh fracture of the ceramic body for comparison. In the case of the bichrome samples from Iasos (IA1, IA5, IA6, IA9, IA10, IA14, and IA15), three measurements were taken on both the black and the red gloss. Similarly, samples presenting an irregular black or red gloss were measured with three individual points on each colour shade (black, grey, brown, or red).

### Scanning electron microscopy coupled with energy-dispersive X-ray spectroscopy

The chemical composition of the samples’ gloss was measured by scanning electron microscopy coupled with energy-dispersive X-ray spectroscopy (SEM-EDS). Twenty of the 47 sherds were selected for SEM-EDS analyses. Fifteen of these have only a black gloss, 2 of them have only a red gloss, and 3 of them are bichrome (see Table 2). This selection was based on the petrographic and mineralogical results obtained beforehand to represent the different petrographic fabrics of each archaeological site and to investigate the diverse diffraction patterns obtained with  $\mu$ -XRD<sup>2</sup>. Furthermore, it was ensured that this sub-selection of samples represented the variety of surface finishes present in the assemblage.



A small cross-section of the selected sherd was cut and embedded in a resin block and gradually polished until a final polishing of 1- $\mu$ m grain size. Lastly, a carbon coating was applied to the sample using a Bal-Tec SCD005 Sputter Coater.

Measurements were performed at the Institute of Archaeology at the University College London using a Carl Zeiss EVO25 electron microscope with a W-filament housed in a Lab-6 column electron generator. The instrument is equipped with an Everhart-Thornley secondary electron detector coupled with a 5 quadrant HD LM 5SBSD-1kV 16-mm low-kV diode back-scattered electron detector. An Oxford Instruments X-Max 80 spectrometer is attached to the microscope to detect the characteristic X-rays. The elemental compositions of the ceramic bodies were measured at 200 $\times$  magnification, while the measurements of the gloss layers were done at 500 $\times$  magnification. The analytical parameters involved an electron beam of 10keV, 2048 channels, and a processing time of 4, with a count limit of 750,000 counts. The acquisition of the spectra, the elements' confirmation, and the quantification were performed with the AZtec 5.0 software provided by Oxford Instruments. At the beginning of each measurement session, a standard measurement was run using the BHVO-2 basalt reference (Wilson 1997) to ensure the quality of the following analyses (see Supplementary data).

For each sample, the elemental composition of the gloss was measured in three different points for both the outer and the inner gloss, or the black and the red gloss respectively, for a total of at least six gloss measurements per sample. Additionally, each sample's ceramic body was measured three times at different points. The original quantifications were performed as non-normalised (see Supplementary Materials). These measurements were then normalised (see Supplementary Materials), and finally, each sample was described with an average elemental composition based on a mean of the measurements taken. However, a few measurements were discarded before calculating the average compositions, as they appeared too different from the other measurements of their respective sample. In addition to the chemical characterisation, BSE micrographs of each measurement area were taken.

## Results

### Characterisation of the ceramic bodies

#### Manfria

The petrographic study of the Manfria assemblage revealed that the black gloss ware could be divided into three petrographic fabrics.

Fabric Ma-A (Fig. 1a) is represented by a non-calcareous fine matrix, weakly bimodal, and of low optical activity, with the common presence of quartz and feldspars, and

occurrence of biotite, muscovite, and iron-rich minerals. Additionally, calcite-rich microfossils were observed in several samples. This fabric includes samples M1, M20, M31, and M40.

Fabric Ma-B (Fig. 1b) is a non-calcareous fine fabric, weakly bimodal, and of medium optical activity, with frequent occurrence of quartz and feldspars, and the presence of calcite, iron-rich minerals, muscovite, and biotite. This fabric includes samples M19 and M42.

Fabric Ma-D (Fig. 1c) is characterised by a very fine non-calcareous paste, unimodal, and with low to non-visible optical activity. It is dominated by quartz inclusions and further contains muscovite, biotite, iron-rich minerals, and calcite. This fabric includes samples M11, M17, M22, M26, M29, M33, M34, and M51.

The PCA of the ceramic body chemical characterisation, which accounts for 66% of the total variation, displays the distribution of the samples into three distinct clusters (Fig. 1d). The samples of fabric Ma-D are separated from the other two fabrics along PC1. This separation is illustrated again in the scatterplot of CaO against SiO<sub>2</sub> (Fig. 1f). This coincides with the petrographic analysis, which identified the presence of micro-fossils and calcite inclusions in fabric Ma-A and Ma-B, respectively, whereas samples of fabric Ma-D are relatively calcite-poor. Additionally, the biplot of Zr vs Ba concentrations (Fig. 1g) displays a chemical differentiation of fabrics Ma-A and Ma-B, which confirms their distinction. In this scatterplot, samples from Ma-B show higher Zr and lower Ba concentrations than samples from Ma-A. Overall, the three fabrics identified via ceramic petrography were confirmed by the bulk chemical analysis.

#### lasos

All samples were already studied and characterised in a previous paper (Amicone 2015), which identified three distinctive petrographic fabrics among the 15 sherds.

Fabric Ia-1 (Fig. 2a) is represented by a non-calcareous reddish clay matrix with small quartz and polycrystalline inclusions and the rare occurrence of biotite and muscovite. This fabric includes 8 samples (IA1, IA2, IA4, IA6, IA9, IA11, IA14, and IA15).

Fabric Ia-2 (Fig. 2b) is characterised by a non-calcareous grey clay matrix with small quartz inclusions and the rare presence of micrite, muscovite, and plagioclase. No provenance was proposed for this fabric, as the scarcity and size of the inclusions do not permit a clear comparison with geological references. This fabric includes 3 samples (IA5, IA8, and IA13).

Lastly, Fabric Ia-3 (Fig. 2c) is characterised by a reddish-brown clay matrix with abundant quartz and muscovite inclusions; the rare presence of feldspar, micrite, and biotite;

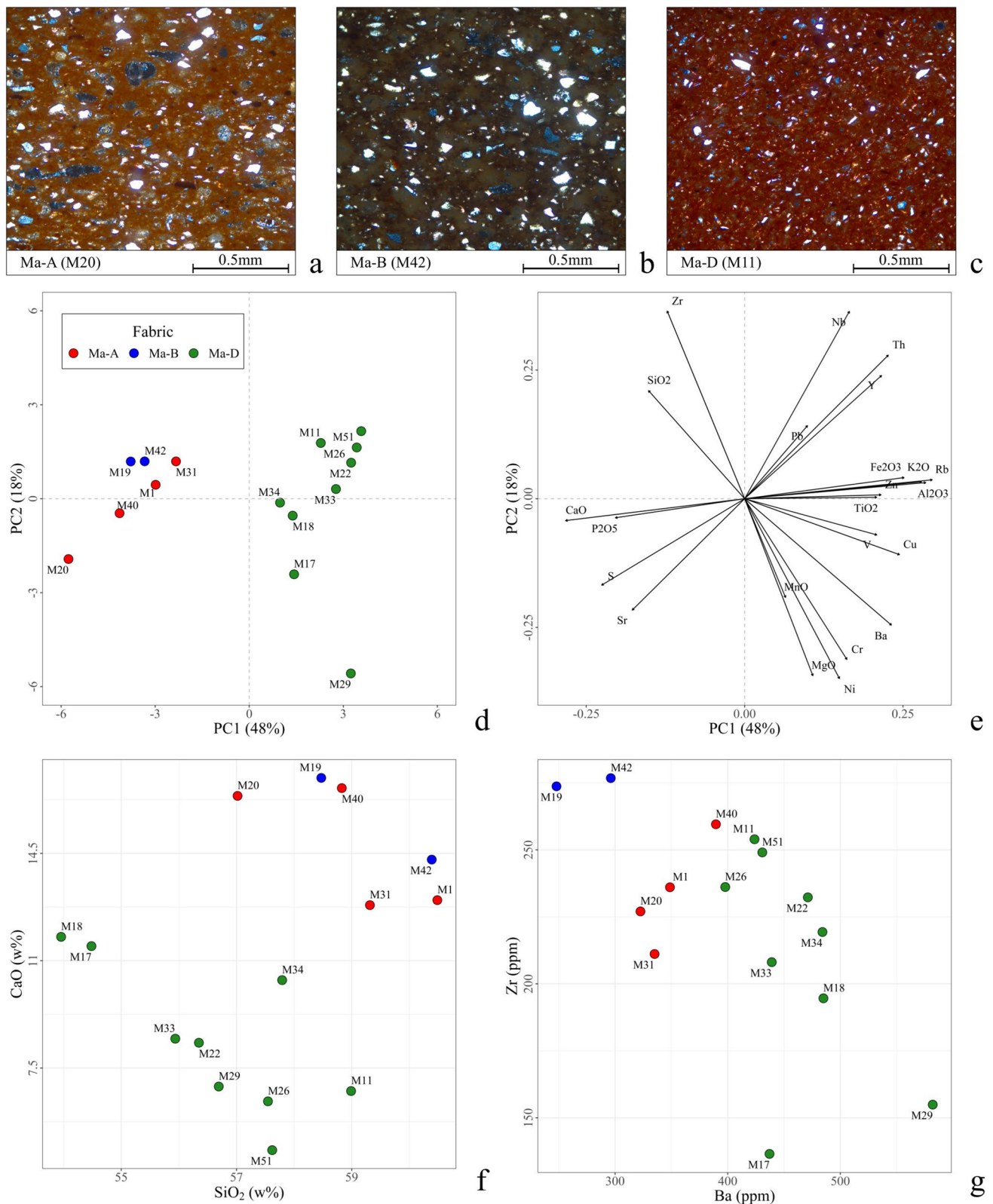


**Fig. 1** **a–c** Petrographic fabrics of Manfria (XP light, field of view 1.5mm). **d–g** Scatterplot and variable plot of the first two principal components of the PCA and bivariate scatterplots based on the pXRF data of the bulk chemical composition of the samples from Manfria

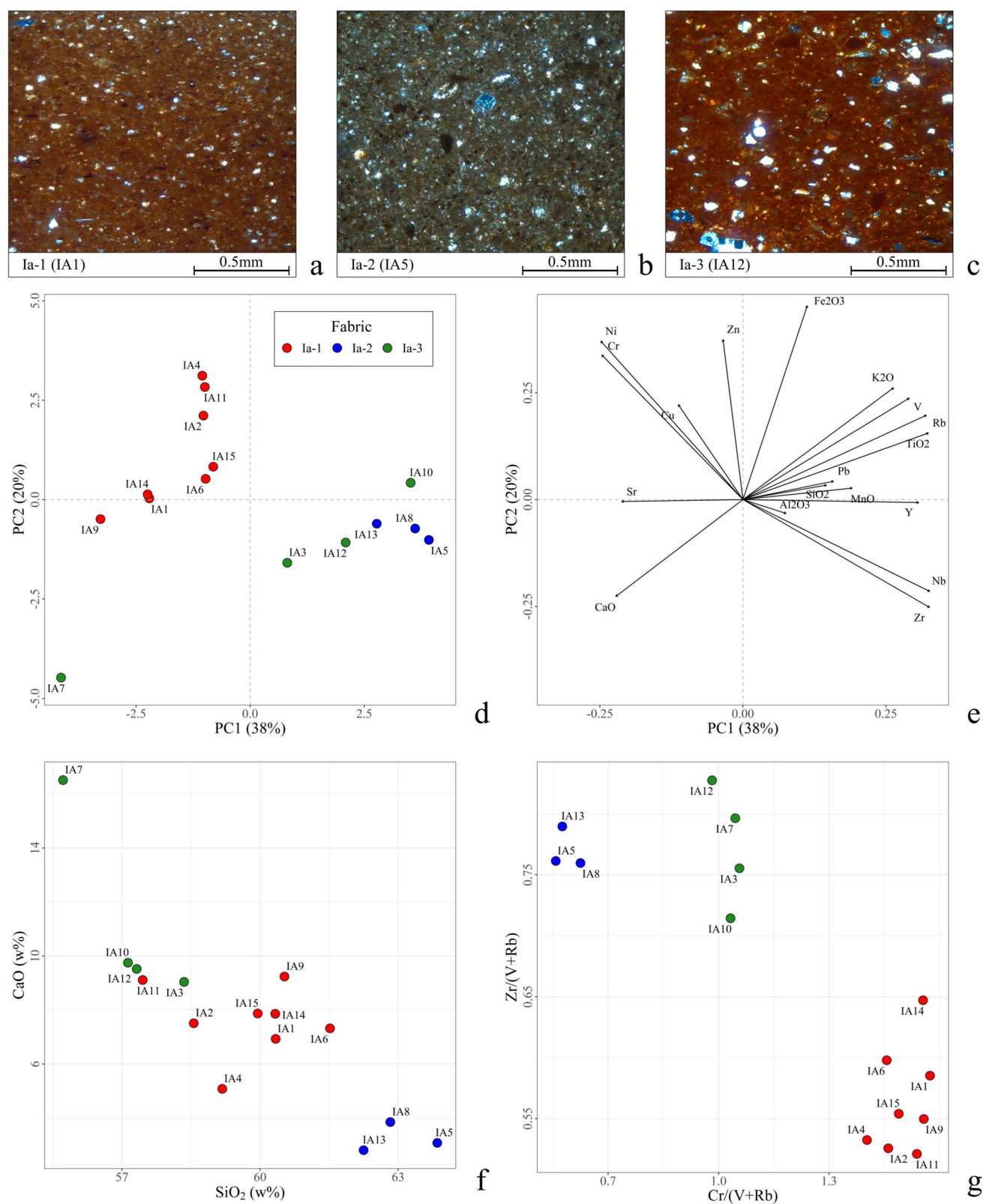


**Fig. 2** a–c Petrographic fabrics of Iasos (XP light). d–g Scatterplot and variable plot of the first two principal components of the PCA and bivariate scatterplots based on the pXRF data of the bulk chemical composition of the samples from Iasos. Chemical data from Amicone (2015)



and the occasional occurrence of metamorphic rock fragments. Some of the samples also bear fragments of shells and clay-rich inclusions. Due to the occurrence of metamorphic inclusions, it was proposed that those sherds could come from the area of modern-day Milas, i.e. the ancient city of Mylasa, located appr. 20 km inland from Iasos, where metamorphic formations are observed (Amicone 2015; Konak and Şenel 2002). Mylasa was an important urban centre and functioned as capital of Caria before the reign of Mausolus. This fabric includes 4 samples (IA3, IA7, IA10, and IA12).

The results of this petrographic study were complemented and confirmed by a chemical characterisation of each sample's ceramic body by pXRF. The PCA (Fig. 2d), which accounts for 58% of the total variation in composition, suggests a clear separation of fabric Ia-1 from the other two fabrics. Moreover, as two samples of fabric Ia-1 were used as Attic reference vases (IA4 and IA11), it was concluded that these 8 samples could represent fourth century BCE Attic imports at Iasos, while the other two fabrics Ia-2 and Ia-3 reflect Atticising productions (Amicone 2015). Given the chemical variability in the samples of fabric Ia-1 in the PCA scatterplot, it could be argued that this fabric can be subdivided. However, as this study aims to compare Attic with Atticising productions, fabric Ia-1 will be kept as one entity. One sample, IA7, plots as an outlier of fabric Ia-3 in the PCA. This can be explained by its very high CaO content (16.51%) compared to the other samples from this site (7.07% on average), as well as by its low V and Rb levels (101 and 120 ppm respectively). This high CaO content (Fig. 2f) can be explained by secondary calcite deposition, which was observed during the petrographic analysis. Furthermore, the scatterplot of  $\text{Cr}/(\text{V}+\text{Rb})$  vs  $\text{Zr}/(\text{V}+\text{Rb})$  (Fig. 2g) corrects for the high vanadium and rubidium levels of sample IA7, making this sherd cluster with the rest of the sample from fabric Ia-3. Thus, this sample can still be considered part of fabric Ia-3. This scatterplot also illustrates that fabrics Ia-2 and Ia-3 can be chemically distinguished by their Cr and Zr contents (Fig. 2g).

## Priene

A total of six distinctive petrographic fabrics were identified by the petrographic analysis of the Priene assemblage.

Fabric Pri-A (Fig. 3a) includes the most samples with 6 specimens: Pri540, Pri544, Pri545, Pri546, Pri552, and Pri571. It is characterised by a non-calcareous clay matrix, reddish to light brown in colour, except for sample Pri545, which has a grey clay matrix. Inclusions are dominated by quartz and muscovite, with presence of amphibole and very small serpentinite inclusions. Few calcite-rich inclusions, most probably microfossil shells, along with shell-shaped voids, are visible in those samples. Sample Pri552 presents big fragments of mica schists.

Fabric Pri-B (Fig. 3b) includes samples Pri533 and Pri534. Its inclusions are dominated by quartz and muscovite, with a few small polycrystalline inclusions, possibly metamorphic rocks, in a reddish non-calcareous clay matrix.

Fabric Pri-C (Fig. 3c) includes samples Pri561 and Pri562. It is defined by a calcareous cream-coloured clay matrix. The quartz and muscovite inclusions in this fabric are less abundant and the quartz grains are coarser than in the other fabrics.

Fabric Pri-D (Fig. 3d) includes samples Pri558 and Pri559. It is characterised by a calcareous cream-coloured clay matrix, with inclusions dominated by fine quartz and muscovite. Few small serpentinite inclusions can be observed as well. Interestingly, both the samples forming this fabric Pri-D have intentional red gloss layers.

Fabric Pri-E (Fig. 3e) includes samples Pri530, Pri602, Pri609, and Pri674. It is characterised by a non-calcareous clay matrix. The colour of the clay is either deep red (samples Pri530 and Pri609) or greyish (sample Pri602). Sample Pri674 presents a mostly greyish matrix, with deep red areas on the outside of the sample. The inclusions are dominated by quartz and muscovite, and quartz inclusions are coarser in this fabric than in others. Few small serpentinite inclusions can be identified as well.

Fabric Pri-F (Fig. 3f) is only represented by sample Pri536. It is similar to fabric Pri-A, characterised by a non-calcareous reddish clay matrix with fine quartz and muscovite inclusions. The placement of sample Pri536 in a separate fabric is discussed in more detail in the following paragraphs and in the 'Petrographic fabrics and production centres' section.

The results of this petrographic study were compared to the chemical characterisation of the samples' ceramic bodies via pXRF. The PCA (Fig. 3g) accounts for 55% of the total variation and shows a good separation of the calcareous fabric Pri-C and Pri-D, which confirms their distinction from the rest of the assemblage. This distinction in calcite content is further visible in the scatterplot of CaO vs  $\text{Fe}_2\text{O}_3$  (Fig. 3i). Additionally, the outlier sample Pri536, representing Pri-F, plots in all 3 scatterplots away from fabric Pri-B, which confirms the differentiation between those two fabrics. In the PCA, Pri-E appears as distinctive from the others along PC1 but separates itself into two groups along PC2. This division of the Pri-E samples can also be observed in the scatterplot of CaO vs  $\text{Fe}_2\text{O}_3$  according to their iron content. This appears connected to the colour of the clay matrix in those samples, as observed in the petrographic analysis, and could suggest a separation of fabric Pri-E into two sub-fabrics. However, for simplification, this fabric still includes all 4 samples in this work. Additionally, samples Pri571 (fabric Pri-A) and Pri609 (fabric Pri-E) appear to separate themselves from their respective fabrics with higher CaO levels than their counterparts (Fig. 3i). This can be explained by

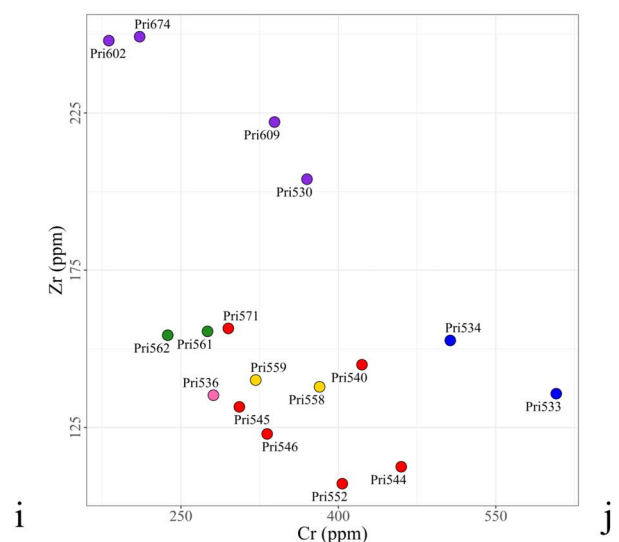
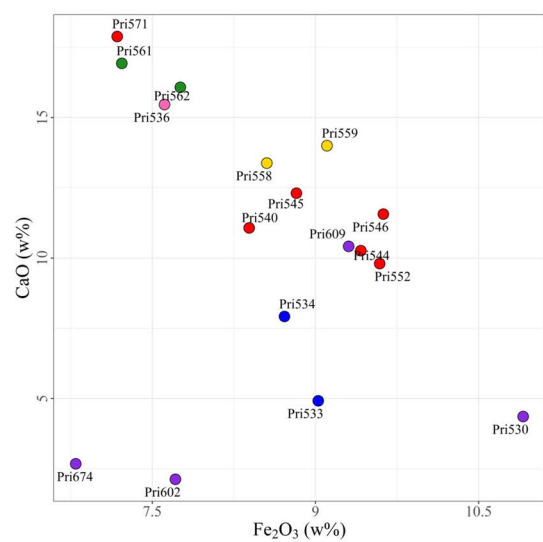
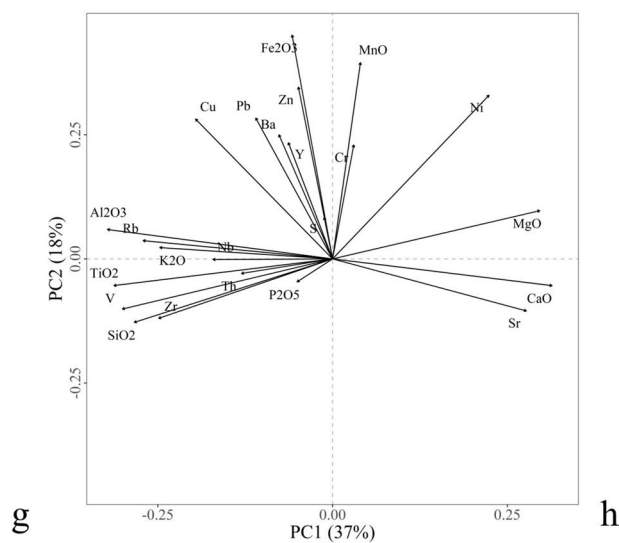
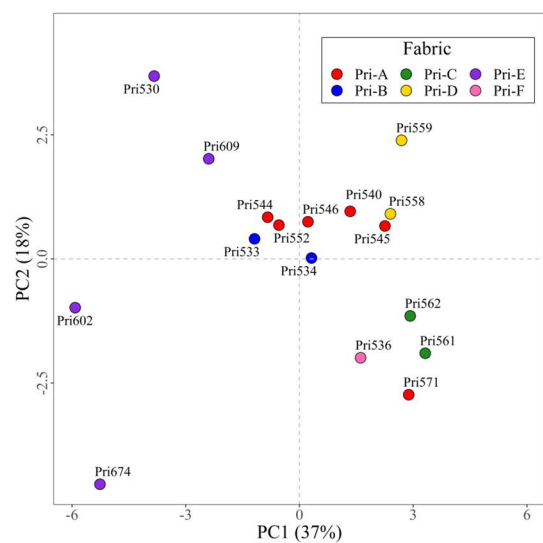
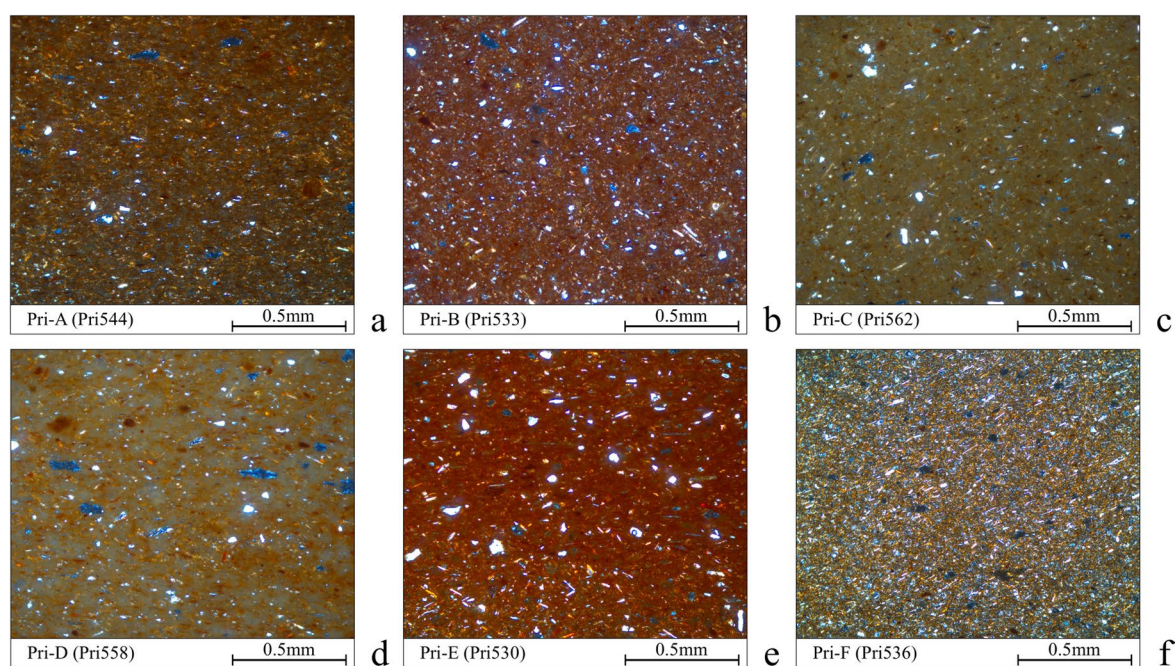


**Fig. 3** a–f Petrographic fabrics of Iasos (XP light). g–j Scatterplot and variable plot of the first two components of the PCA and bivariate scatterplots based on the pXRF data of the bulk chemical composition of the samples from Iasos. Chemical data from Heinze (2023)

the presence of secondary calcite deposition, which was observed in those two samples during the petrographic analysis. Therefore, these two specimens are still considered part of their respective fabrics. Lastly, scatterplots of CaO vs Fe<sub>2</sub>O<sub>3</sub> and Cr vs Zr demonstrate the separation of fabric Pri-B from the others with low CaO and Zr levels and high Cr contents (Fig. 3i–j). Overall, the separation of the assemblage in 6 petrographic fabrics was visually confirmed by the PCA and bivariate scatterplots.

### Gloss chemical characterisation by SEM-EDS

The chemical characterisation of the 18 black gloss specimens reveals a relatively homogeneous composition (Table 3 and Fig. 4), corresponding to a typical vitrified clay slip, with a relatively high Al<sub>2</sub>O<sub>3</sub> level compared to their SiO<sub>2</sub> content with an average of 29.9% and 44.9% respectively. Furthermore, they all appear to have relatively high FeO (14.9%) and K<sub>2</sub>O (5.5%) levels and a low CaO content (1.1%). The Na<sub>2</sub>O and P<sub>2</sub>O<sub>5</sub> contents are also relatively homogeneous with respective averages of 0.7% and 0.3%. Interestingly, a rather high ZnO content was detected in two of the black gloss specimens (M42 and Pri533), with 0.3% and 0.4% respectively.

Despite an overall homogeneity of the data, some variations in the chemical composition were observed. Sample IA10 displays high CaO (8.9%) and P<sub>2</sub>O<sub>5</sub> (0.6%) contents (Fig. 4b–c). Nevertheless, it can be argued that these values should be considered with caution, as they have higher standard deviations than the measurements of other samples (Table 3). Black gloss Pri562 shows a high K<sub>2</sub>O content (11.4%), much higher than the other black gloss specimens (5.5% on average) (Fig. 4a), which is discussed in the ‘Black gloss raw material’ section. Other samples (Pri540, IA4, M1, and M42) also appear to have high absolute K<sub>2</sub>O levels (all higher than 6.5%) but exhibit similar overall ratios of potassium to the clayey fraction (alumina + silica) to the rest of the black gloss assemblage (Fig. 4a), and therefore can be considered comparable with the rest of the assemblage. Lastly, sample IA6 exhibits a much higher Al<sub>2</sub>O<sub>3</sub>/SiO<sub>2</sub> ratio (Fig. 4b), which does not appear to come from measurement errors and is further discussed in the ‘Black gloss raw material’ section.

The red gloss chemical characterisation of the 4 bichrome vessels from Iasos (IA1, IA6, IA10, and IA13) and the 2 intentional red gloss vessels of Priene (Pri558 and Pri571) have an overall similar composition compared to the analysed black gloss samples (Table 3). Nonetheless, variations can be observed in the chemical composition of the red gloss samples. Sample Pri558 has a higher K<sub>2</sub>O (9.5%)

content and a slightly higher Na<sub>2</sub>O/(Al<sub>2</sub>O<sub>3</sub>+SiO<sub>2</sub>) ratio than the black gloss samples. Red gloss specimens Pri571, IA10, and IA13 have a high content of CaO (1.8%, 2.3%, and 2.0% respectively). IA10 is also characterised by very high sodium levels (1.9%). Lastly, IA1 displays quite high phosphorus levels, but with an equally high standard deviation, which suggests that this value should be taken with caution. A more detailed description of the chemical variations between black and red gloss decorations is discussed in the ‘Technological relationship between black and red gloss’ section.

### Gloss mineralogical characterisation by $\mu$ -XRD<sup>2</sup>

The black gloss mineralogical characterisation reveals the presence of reduced iron oxides in the assemblage. Both magnetite and hercynite are detected in different intensities in the various specimens with their main diffraction peak at around 41.4°2 $\theta$  ( $d = 2.53\text{\AA}$ ) and 42.7°2 $\theta$  ( $d = 2.46\text{\AA}$ ) respectively (Fig. 5a–c). Due to the overlap and the broad intensities,  $\mu$ -XRD<sup>2</sup> does not allow for a clear distinction between magnetite and maghemite (detected at around 41.6°2 $\theta$ ,  $d = 2.52\text{\AA}$ ), but it can be assumed that maghemite is also present beside magnetite in most of the gloss specimens. Additionally, the red, oxidised iron oxide hematite is detected by its main reflection at 38.7°2 $\theta$  ( $d = 2.70\text{\AA}$ ) in a few samples. The analyses of the brown areas of the irregular black gloss specimens indicate the presence of mostly hematite and maghemite and/or magnetite (Fig. 5a–c).

The characterisation of the red gloss ware from Iasos shows that their iron oxide phase is dominated by hematite together with magnetite/maghemite (Fig. 5d). A very small peak of hercynite can also be observed in most of these gloss’ diffractograms. Similarly, the intentional red gloss specimens of Priene display the presence of hematite and maghemite and/or magnetite. In these samples, however, no hercynite can be detected.

The measurements also exhibit the presence of quartz together with feldspars in most of the gloss specimens. Although these minerals can be present in the gloss itself, part of the signal presumably comes from the underlying ceramic body, as the X-rays penetrate a little deeper than the thickness of the gloss. As for the iron oxides contained in the ceramic body, the control measurements of the ceramic bodies do show the presence of some iron oxides, but in a much lesser intensity than in their respective gloss, verifying the validity of gloss measurements.

### Microstructure observations by SEM

The BSE micrographs of the gloss layers taken via SEM allowed for a visual evaluation of their microstructure (Fig. 6). While most samples display a dense and



**Table 3** Mean chemical composition of each black and red specimen's gloss calculated from the normalised quantification of the multiple measurements performed on each sample by SEM-EDS. n: number of measurements; SD standart deviation; –, element not detected

| Sample      | Na <sub>2</sub> O | MgO  | Al <sub>2</sub> O <sub>3</sub> | SiO <sub>2</sub> | P <sub>2</sub> O <sub>5</sub> | SO <sub>3</sub> | Cl   | K <sub>2</sub> O | CaO | TiO <sub>2</sub> | Cr <sub>2</sub> O <sub>3</sub> | MnO | FeO | ZnO  | n    |      |   |   |
|-------------|-------------------|------|--------------------------------|------------------|-------------------------------|-----------------|------|------------------|-----|------------------|--------------------------------|-----|-----|------|------|------|---|---|
| Black gloss | M1                | Mean | 1.0                            | 1.8              | 29.0                          | 45.1            | 0.2  | 0.1              | –   | 6.9              | 1.2                            | 0.5 | 0.1 | 0.1  | 14.0 | –    | 6 |   |
|             |                   | SD   | 0.1                            | 0.1              | 0.7                           | 0.7             | 0.1  | 0.0              | –   | 0.2              | 0.2                            | 0.0 | 0.0 | 0.1  | 0.6  | –    |   |   |
|             | M11               | Mean | 0.9                            | 1.9              | 29.7                          | 45.7            | 0.2  | 0.2              | 0.1 | 4.8              | 1.2                            | 0.5 | 0.1 | 0.2  | 14.7 | –    | 5 |   |
|             |                   | SD   | 0.1                            | 0.1              | 0.3                           | 0.7             | 0.0  | 0.1              | –   | 0.1              | 0.2                            | 0.1 | –   | 0.0  | 1.0  | –    |   |   |
|             | M17               | Mean | 0.5                            | 1.7              | 30.5                          | 45.9            | 0.2  | 0.1              | –   | 4.6              | 1.1                            | 0.6 | 0.1 | 0.2  | 14.5 | –    | 6 |   |
|             |                   | SD   | 0.1                            | 0.1              | 0.2                           | 0.2             | 0.1  | 0.0              | –   | 0.8              | 0.5                            | 0.1 | 0.0 | 0.1  | 0.3  | –    |   |   |
|             | M26               | Mean | 0.4                            | 1.7              | 29.9                          | 45.1            | 0.2  | 0.1              | 0.1 | 5.0              | 0.8                            | 0.6 | 0.1 | 0.1  | 16.1 | –    | 6 |   |
|             |                   | SD   | 0.1                            | 0.1              | 0.2                           | 0.2             | 0.1  | 0.1              | –   | 0.2              | 0.1                            | 0.0 | 0.1 | 0.0  | 0.3  | –    |   |   |
|             | M31               | Mean | 0.6                            | 2.3              | 27.8                          | 45.1            | 0.2  | 0.2              | 0.1 | 6.4              | 1.2                            | 0.7 | 0.1 | 0.1  | 15.4 | –    | 6 |   |
|             |                   | SD   | 0.1                            | 0.1              | 0.9                           | 2.1             | 0.1  | 0.1              | –   | 0.6              | 0.2                            | 0.1 | 0.0 | 0.0  | 2.2  | –    |   |   |
|             | M42               | Mean | 1.1                            | 1.6              | 30.6                          | 44.6            | 0.1  | 0.2              | 0.1 | 6.8              | 1.0                            | 0.5 | 0.1 | 0.1  | 13.1 | 0.4  | 6 |   |
|             |                   | SD   | 0.2                            | 0.1              | 0.9                           | 1.4             | 0.1  | 0.0              | 0.2 | 0.5              | 0.2                            | 0.1 | 0.0 | –    | 2.0  | 0.1  |   |   |
|             | IA1               | Mean | 0.5                            | 1.9              | 30.2                          | 46.8            | 0.2  | 0.3              | 0.3 | 3.9              | 0.8                            | 0.7 | –   | –    | 14.5 | –    | 3 |   |
|             |                   | SD   | 0.1                            | 0.0              | 0.1                           | 0.1             | 0.1  | 0.1              | 0.1 | 0.1              | 0.0                            | 0.0 | –   | –    | 0.2  | –    |   |   |
|             | IA4               | Mean | 0.4                            | 1.6              | 29.7                          | 42.8            | 0.3  | 0.1              | –   | 7.6              | 1.4                            | 0.4 | 0.1 | 0.1  | 15.7 | –    | 6 |   |
|             |                   | SD   | 0.1                            | 0.1              | 0.4                           | 0.5             | 0.1  | –                | –   | 0.3              | 0.5                            | 0.1 | 0.0 | 0.0  | 0.1  | –    |   |   |
|             | IA6               | Mean | 0.7                            | 2.2              | 32.1                          | 40.9            | 0.4  | 2.2              | 0.1 | 2.6              | 1.5                            | 0.9 | 0.1 | 0.1  | 16.4 | –    | 3 |   |
|             |                   | SD   | 0.1                            | 0.1              | 0.5                           | 0.3             | 0.1  | 0.3              | 0.0 | 0.1              | 0.1                            | 0.1 | 0.0 | 0.0  | 0.1  | –    |   |   |
|             | IA10              | Mean | 0.8                            | 2.2              | 28.5                          | 44.6            | 0.6  | 0.2              | 0.5 | 4.2              | 2.9                            | 0.6 | 0.1 | 0.2  | 14.8 | –    | 3 |   |
|             |                   | SD   | 0.1                            | 0.1              | 0.7                           | 0.3             | 0.5  | 0.1              | 0.2 | 0.1              | 0.8                            | 0.0 | 0.0 | 0.1  | 0.4  | –    |   |   |
| Black gloss | IA13              | Mean | 1.3                            | 1.5              | 29.4                          | 44.3            | 0.2  | –                | –   | 5.6              | 0.9                            | 0.7 | 0.1 | 0.2  | 15.7 | –    | 3 |   |
|             |                   | SD   | 0.0                            | 0.0              | 0.3                           | 0.2             | 0.1  | –                | –   | 0.0              | 0.1                            | 0.0 | 0.0 | 0.1  | 0.3  | –    |   |   |
|             | Pri530            | Mean | 0.6                            | 1.7              | 30.4                          | 45.4            | 0.3  | 0.2              | –   | 4.2              | 0.9                            | 0.5 | 0.1 | 0.2  | 15.4 | –    | 5 |   |
|             |                   | SD   | 0.2                            | 0.0              | 0.7                           | 1.1             | 0.0  | 0.1              | –   | 0.6              | 0.4                            | 0.1 | –   | 0.1  | 0.4  | –    |   |   |
|             | Pri533            | Mean | 0.4                            | 1.7              | 31.5                          | 45.9            | 0.3  | 0.1              | –   | 4.4              | 0.4                            | 0.5 | 0.1 | 0.1  | 14.9 | 0.3  | 6 |   |
|             |                   | SD   | 0.1                            | 0.1              | 0.4                           | 0.8             | 0.1  | 0.0              | –   | 0.2              | 0.1                            | 0.1 | 0.0 | 0.0  | 0.8  | –    |   |   |
|             | Pri536            | Mean | 0.6                            | 1.6              | 31.5                          | 45.7            | 0.3  | 0.2              | 0.1 | 3.0              | 0.7                            | 0.6 | 0.1 | 0.1  | 15.6 | –    | 3 |   |
|             |                   | SD   | 0.1                            | 0.1              | 0.3                           | 0.6             | 0.1  | 0.2              | –   | 0.3              | 0.3                            | 0.0 | 0.0 | 0.0  | 1.3  | –    |   |   |
|             | Pri540            | Mean | 1.1                            | 1.9              | 29.0                          | 44.6            | 0.2  | 0.1              | 0.1 | 8.4              | 0.8                            | 0.5 | 0.1 | 0.1  | 13.2 | –    | 5 |   |
|             |                   | SD   | 0.5                            | 0.1              | 0.5                           | 0.9             | 0.1  | 0.1              | –   | 0.6              | 0.4                            | 0.0 | –   | 0.0  | 0.6  | –    |   |   |
|             | Pri544            | Mean | 0.2                            | 1.8              | 29.7                          | 44.7            | 0.3  | 0.1              | –   | 4.2              | 0.5                            | 1.1 | 0.1 | 0.1  | 17.3 | –    | 4 |   |
|             |                   | SD   | 0.1                            | 0.1              | 0.4                           | 0.6             | 0.1  | 0.1              | –   | 0.8              | 0.3                            | 0.0 | 0.0 | 0.0  | 0.2  | –    |   |   |
|             | Pri562            | Mean | 0.6                            | 1.7              | 27.9                          | 42.4            | 0.3  | 0.1              | 0.1 | 11.4             | 1.1                            | 0.6 | 0.1 | 0.1  | 13.8 | –    | 6 |   |
|             |                   | SD   | 0.3                            | 0.1              | 1.1                           | 1.6             | 0.1  | 0.0              | 0.0 | 1.8              | 0.7                            | 0.2 | –   | 0.0  | 0.4  | –    |   |   |
|             | Pri602            | Mean | 0.6                            | 2.1              | 30.3                          | 48.2            | 0.3  | 0.2              | 0.1 | 4.5              | 0.5                            | 0.5 | 0.1 | 0.1  | 12.6 | –    | 7 |   |
|             |                   | SD   | 0.2                            | 0.1              | 0.6                           | 1.0             | 0.0  | 0.1              | –   | 0.4              | 0.2                            | 0.1 | 0.0 | 0.0  | 0.6  | –    |   |   |
|             | Red gloss         | IA1  | Mean                           | 0.6              | 2.0                           | 29.5            | 46.0 | 0.5              | 0.1 | 0.2              | 3.9                            | 1.0 | 0.9 | –    | –    | 15.4 | – | 3 |
|             |                   |      | SD                             | 0.0              | 0.1                           | 0.4             | 0.7  | 0.3              | 0.1 | 0.1              | 0.3                            | 0.5 | 0.1 | –    | –    | 0.6  | – |   |
|             |                   | IA6  | Mean                           | 0.8              | 1.9                           | 30.2            | 45.7 | 0.2              | –   | –                | 5.5                            | 0.3 | 0.7 | 0.1  | 0.1  | 14.5 | – | 3 |
|             |                   |      | SD                             | 0.1              | 0.0                           | 0.1             | 0.1  | 0.0              | –   | –                | 0.1                            | 0.0 | 0.1 | 0.0  | 0.0  | 0.1  | – |   |
| IA10        |                   | Mean | 1.9                            | 2.0              | 27.7                          | 42.8            | 0.1  | 0.1              | 0.1 | 7.4              | 2.3                            | 0.6 | 0.1 | 0.2  | 14.7 | –    | 3 |   |
|             |                   | SD   | 0.0                            | 0.1              | 0.2                           | 0.2             | 0.0  | 0.0              | 0.1 | 0.1              | 0.1                            | 0.1 | 0.1 | 0.1  | 0.2  | –    |   |   |
| IA13        |                   | Mean | 0.8                            | 1.7              | 29.2                          | 45.0            | 0.3  | 0.1              | 0.3 | 2.0              | 0.7                            | 0.1 | 0.2 | 16.1 | –    | 3    |   |   |
|             |                   | SD   | 0.0                            | 0.2              | 0.4                           | 0.2             | 0.1  | –                | 0.1 | 0.1              | 0.9                            | 0.1 | 0.1 | 0.0  | 0.3  | –    |   |   |
| Pri558      |                   | Mean | 1.4                            | 1.6              | 29.4                          | 43.2            | 0.2  | 0.2              | –   | 9.5              | 1.3                            | 0.7 | 0.1 | 0.1  | 12.6 | –    | 6 |   |
|             |                   | SD   | 0.1                            | 0.2              | 0.3                           | 0.7             | 0.1  | 0.1              | –   | 0.1              | 0.6                            | 0.2 | 0.0 | –    | 0.8  | –    |   |   |
| Pri571      |                   | Mean | 0.8                            | 1.7              | 29.2                          | 45.0            | 0.3  | 0.1              | 0.3 | 2.0              | 0.7                            | 0.1 | 0.2 | 16.1 | –    | 3    |   |   |
|             |                   | SD   | 0.0                            | 0.2              | 0.4                           | 0.2             | 0.1  | –                | 0.1 | 0.1              | 0.9                            | 0.1 | 0.1 | 0.0  | 0.3  | –    |   |   |

Table 3 (continued)

| Sample | Na <sub>2</sub> O | MgO | Al <sub>2</sub> O <sub>3</sub> | SiO <sub>2</sub> | P <sub>2</sub> O <sub>5</sub> | SO <sub>3</sub> | Cl  | K <sub>2</sub> O | CaO | TiO <sub>2</sub> | Cr <sub>2</sub> O <sub>3</sub> | MnO | FeO  | ZnO | n |
|--------|-------------------|-----|--------------------------------|------------------|-------------------------------|-----------------|-----|------------------|-----|------------------|--------------------------------|-----|------|-----|---|
| Mean   | 1.2               | 1.8 | 27.5                           | 44.4             | 0.3                           | 0.2             | 0.2 | 5.9              | 1.8 | 0.8              | 0.1                            | 0.1 | 15.8 | –   | 6 |
| SD     | 0.0               | 0.1 | 0.3                            | 0.4              | 0.0                           | 0.1             | 0.1 | 0.1              | 0.1 | 0.2              | 0.0                            | 0.1 | 0.0  | 0.7 | – |

homogeneous microstructure with some bloating pores<sup>2</sup> on their surface, others show internal fractures and a higher number of bloating pores at their surface. Red gloss sample Pri571 displays a less compact gloss compared to the other samples, with a darker core. The gloss of sample Pri602 appears most altered with a high heterogeneity, many cracks, and a much thinner gloss than the other samples. This gloss could be qualified as broken and flaky according to the terminology used by Aloupi-Siotis (2020, p. 12).

The thickness of the black gloss layers ranges from 7.5 to 33.3µm (mean 14.3µm), while the red gloss layers range from 9.4 to 23.6µm (mean 15.1µm).

Discussion

Petrographic fabrics and production centres

The Manfredia black gloss assemblage was represented by three fabrics. Fabric Ma-A was marked by the presence of microfossils, fins comparison in the local black gloss production of Gela (Barone et al. 2012, 2017; Ingoglia et al. 2018; Santostefano et al. 2018; Spagnolo et al. 2018). Fabric Ma-B can also be associated with the characteristic calcareous deposits of south-central Sicily (Barbera et al. 2018; Montana et al. 2011) and, therefore, can be considered a local/regional production. Fabric Ma-D, however, cannot be associated with any known Sicilian production (Montana et al. 2011), most probably representing an imported production from outside Sicily. Regarding the pXRF bulk analysis, the chemical proximity of fabrics Ma-A and Ma-B and their good separation with fabric Ma-D can be explained by the fact that both Ma-A and Ma-B represent Sicilian fabrics, and are, therefore, chemically closer compared to fabric Ma-D, which could represent non-Sicilian imports.

As already stated, the black gloss ware from Iasos was divided into three distinctive fabrics, of which fabric Ia-1 can be attributed to the Attic production centres (Amicone

2015). Although the origin of the two other fabrics remains uncertain, it can be assumed that these fabrics represent Atticising productions from the vicinity of Iasos or, more broadly, from Asia Minor.

The black gloss assemblage of Priene was divided into six distinctive petrographic fabrics. Fabric Pri-A comprises vessels considered local or regional from Heinze’s work (2023), due to the presence of macroscopically visible snail shell fragments. These were also observed in the present petrographic study. Furthermore, the presence of mica shist fragments, already associated with the local cooking ware productions in Priene (Amicone et al. 2014, 2023), has been observed in this fabric, confirming its local/regional origin. In thin section, fabric Pri-B showed a close similarity to fabric Ia-1, suggesting its Attic origin. This is further supported by the fact that the vessels from fabric Pri-B were typologically and stylistically (i.e., via the stamps used for the decoration) attributed to Attic productions (Heinze 2014). No conclusions could be drawn regarding the provenance of fabric Pri-C and Pri-D. However, it is clear that these vessels were Atticising, as both fabrics are highly calcareous, a feature that is not observed in traditional Attic black gloss pottery (Aloupi-Siotis 2008). It can therefore reasonably be assumed that these fabrics represent Atticising productions from Asia Minor. The four vessels constituting fabric Pri-E were previously suggested through typology to be Knidian imports based on macroscopic observations, which showed similarity with a ‘black-slipped Knidian fabric’ found in Halicarnassus (Vaag et al. 2002). Finally, fabric Pri-F, composed of only one sample (Pri536), presented similarity with the Attic fabric Pri-B. Nevertheless, the chemical characterisation of the ceramic bodies confirmed that fabric Pri-B and Pri-F cannot represent a similar production. Furthermore, the shape of the bolsal Pri536 was identified as non-Attic, again confirming the distinction.

Overall, the studied vessels are characterised by a high degree of clay refinement through the use of refined clays to shape the ceramic bodies. This treatment of the raw material for the ceramic body appears consistent with previous observations on Attic and Atticising pottery (Aloupi-Siotis 2020, Mirti et al. 1996). Nonetheless, the variability in the use of clay types between the different productions shows that the potters did not search for a specific type of clay source to manufacture their ceramic bodies but, rather, used the clay deposits readily available to them.

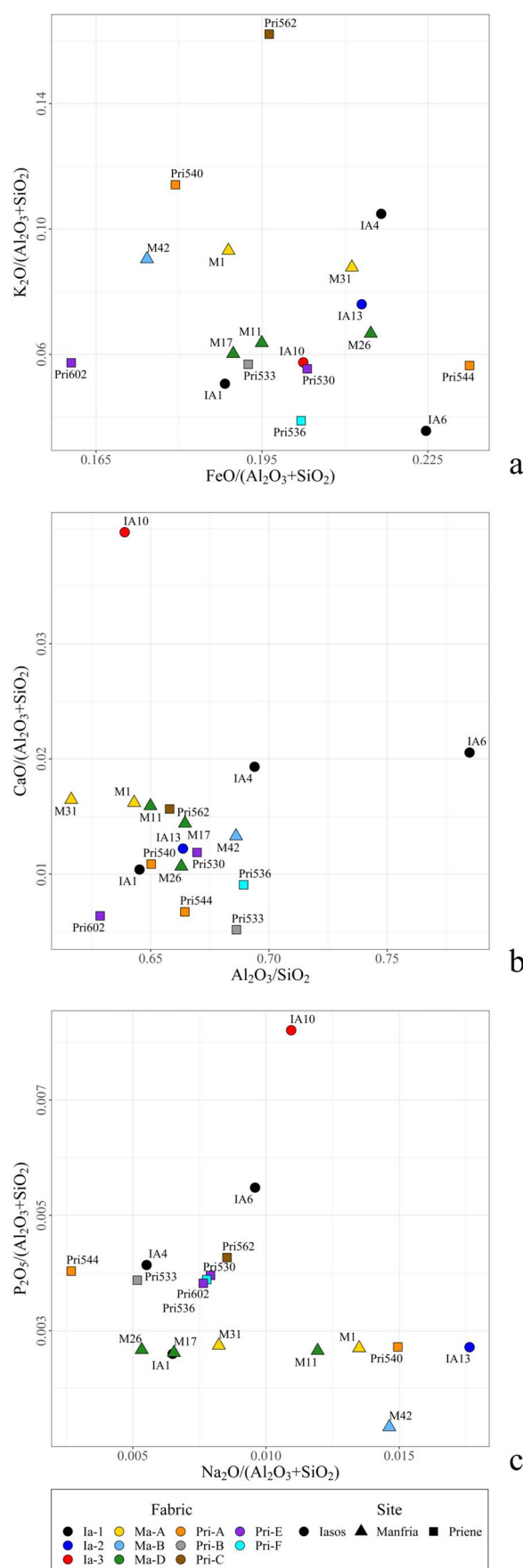
<sup>2</sup> At maximum temperature during the firing, decomposition of organic matter, sulphides, or carbonate causes the production of gases. These gases are trapped in the glassy matrix formed during vitrification and produce spherical bubbles (Aloupi-Siotis 2020; Tite 2007).

**Fig. 4** a–c Scatterplots based on the chemical characterisation of the black gloss samples from Iasos, Manfria, and Priene by SEM-EDS

## Black gloss raw material

In general, this work pointed out that in both Attic and Atticising black gloss productions, similar raw materials for the preparation of the clay paint were used. Indeed, the chemical characterisation of the black gloss vessels from Manfria, Iasos, and Priene indicated mostly low calcite concentrations, along with relatively high amounts of iron-oxide and the presence of  $K_2O$  (associated with the illitic fraction of the clay) in the range of 3 to 6%. These three key points demonstrate that non-calcareous, iron- and illite-rich clays were chosen by both the Attic potters and the producers of Atticising vases for the manufacture of clay paint. As shown in the distribution plots grouping the data of this study with published material (Fig. 7), the Atticising black gloss vessels from Iasos, Manfria, and Priene have very similar chemical compositions to the Attic references. Therefore, it can be assumed that the potters who manufactured these Atticising vessels were able to identify suitable clays to produce successful black gloss ware. Furthermore, the refinement of the clay can be seen in the scatterplot of  $FeO/(Al_2O_3+SiO_2)$  vs  $Al_2O_3/SiO_2$  (Fig. 7a). In this plot, Attic and Atticising black gloss all display high alumina and iron relative contents characteristic of highly refined clays. These observations also demonstrate a similar processing technique of raw material to produce their clay paints.

Nonetheless, variability can be observed in the chemical composition of the gloss layers. Black gloss IA6 showed a high  $Al_2O_3/SiO_2$  ratio, which reflects the degree of refinement of the clay paint. A high ratio in the case of this sample suggests the use of a more refined clay fraction for the manufacture of the clay paint compared to the other gloss of the assemblage. A high  $K_2O$  content was observed in sample Pri562 (11.4%), which could point out the addition of a potassium-rich material, such as potash, by the potter to facilitate the clay suspension process (Hofmann 1962; Noble 1960; Winter 1978). Similarly, the use of soda-rich plant ash or bone ash as deflocculating agents during the preparation of the clay paint could explain the small variation observed in the contents of  $Na_2O$  and  $P_2O_5$  respectively (Aloupi-Siotis 2020; Hofmann 1962; Winter 1978). Additionally, the high  $CaO$  content in sample IA10 (2.9%) could indicate the use of a calcareous-rich clay, instead of a non-calcareous one, which is further supported by the tendency of this sample's gloss to flake, likely related to its high  $CaO$  content (Chaviara and Aloupi-Siotis 2016). However, it cannot be excluded that the chemical variability observed in these few specimens could simply be due to post-depositional processes, which changed the final chemistry of their gloss.



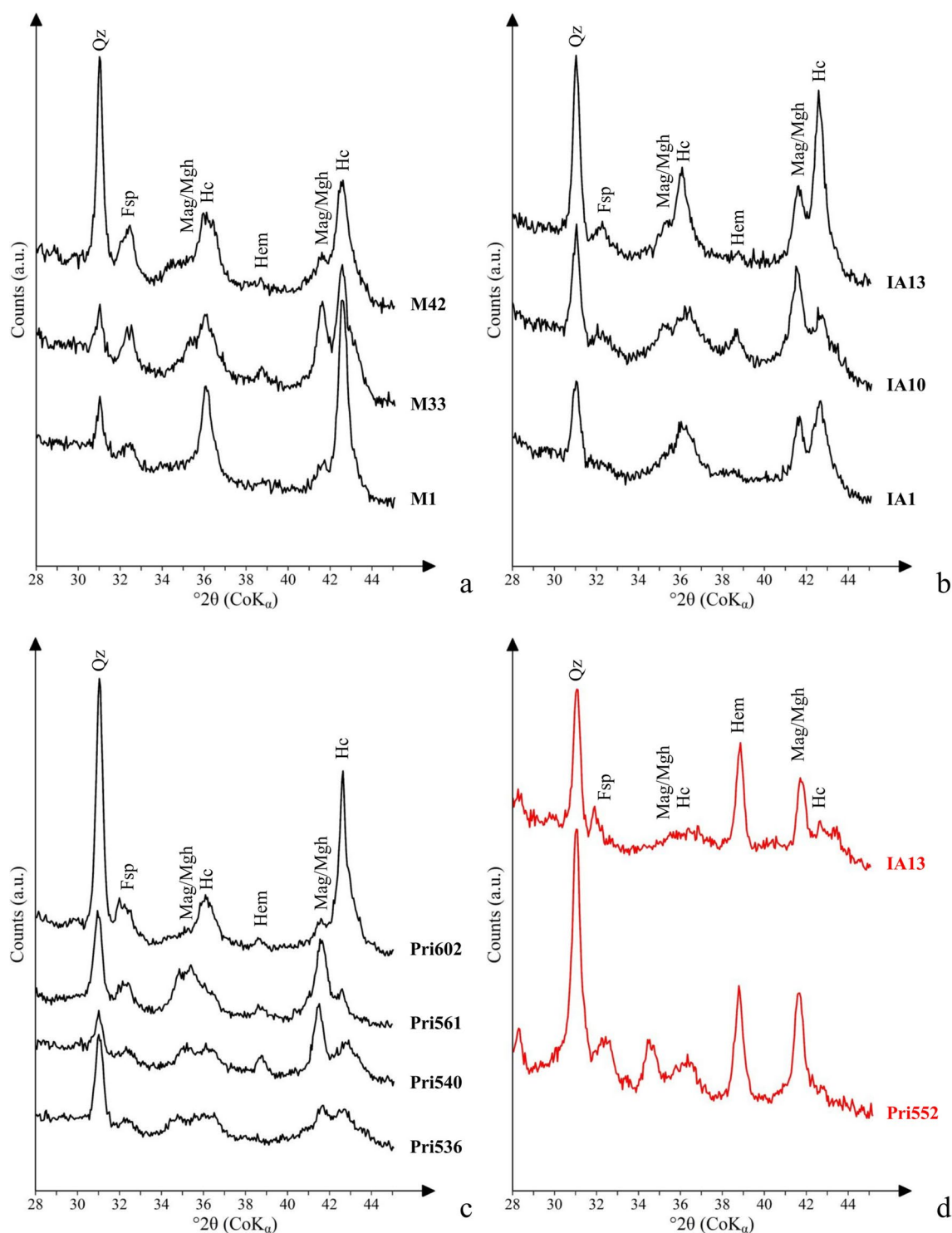


**Fig. 5** Selection of diffractograms of the analysed glass specimens. **a** Black gloss from Manfria. **b** Black gloss from Iasos. **c** Black gloss from Priene. **d** Red gloss from Iasos and Priene

Black gloss M42 and Pri533 were the only two samples of the analysed sample to exhibit the presence of zinc in their gloss layer. As argued by a previous study (Walton et al. 2014), the presence of zinc could mark the use of a

Zn-rich acidic liquid to treat an originally calcareous clay to enhance the dispersion of the clay particles in the water suspension. Yet, another study (Chaviara and Aloupi-Siotis 2016) showed that a substantial zinc content as a trace



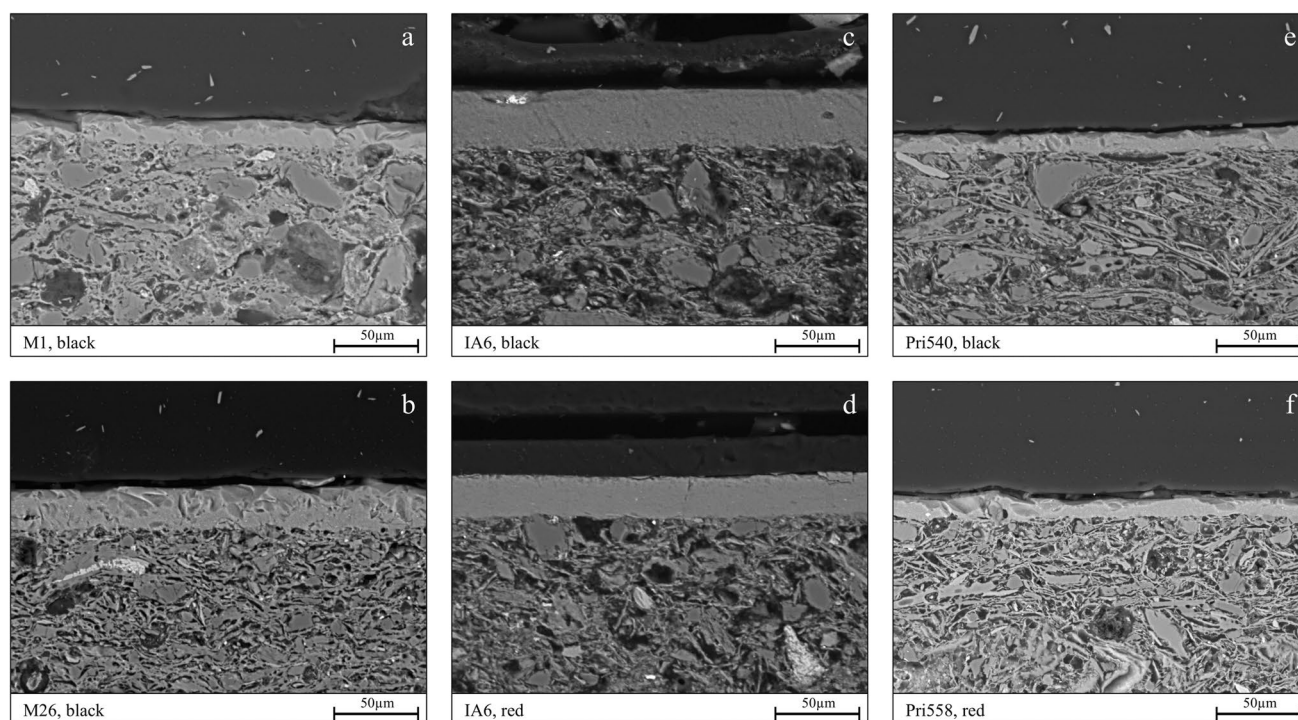


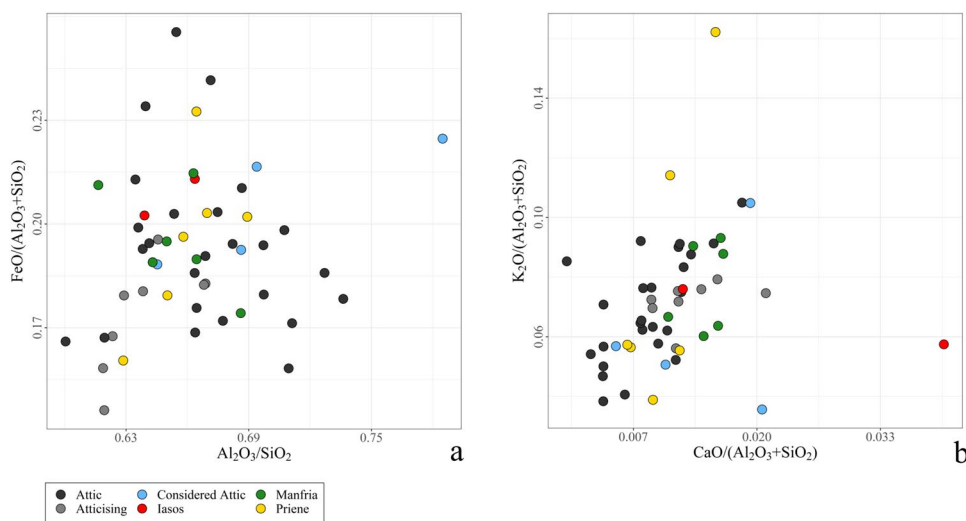
**Fig. 6** a-f BSE Micrographs of black and red gloss layers, magnification  $\times 500$

element simply characterises some ferruginous clay deposits in areas of mining of silver-rich lead ores, such as the Laurion mine in Attica. A recent publication argued that the Zn content in black gloss decorations, in particular the Zn/Ti ratio, could be used to discriminate specific Attic black-figure painters (Muşkara and Kalaycı 2021). Although these different studies give compelling hypotheses for the cause of high Zn content in black gloss, it is not possible to confirm, in the case of M42 and Pri533, if Zn is a potential marker for a clay processing technique or a provenance indicator.

Overall, although chemical variability was observed among the studied gloss specimens, the comparison with the previously published data indicates that these differences are in the range of what is observed in other Attic and Atticising black gloss (see references in Fig. 7).

Nonetheless, the evidence that potters across the Mediterranean used very similar raw materials raises questions regarding the availability of such clay sources in the various regions producing Atticising black gloss. Many clay sources suitable for black gloss production were found in

**Fig. 7** a-b Distribution of the relative composition in major and minor oxides in the black gloss specimens from this study and published data. Attic black gloss data from Kingery 1991; Maniatis et al. 1993; Mirti et al. 1996; Tite et al. 1982; Walton et al. 2009; Atticising black gloss data from Locri, Calabria (Mirti et al. 1996)



Attica (Chaviara and Aloupi-Siotis 2016), and it was suggested that similar red clayey deposits can be found in Mediterranean regions, which result from the deposition of dust storms originating from the Sahara (Avila et al. 1997; Muhs et al. 2010; Rodriguez-Navarro et al. 2018; Yaalon 1997). However, as these local clay deposits are not yet identified nor proven suitable for the production of black gloss, it remains unclear how the local potters procured the raw material. Geological surveys to search for such clay deposits and experimental reproductions to ensure their suitability to produce black gloss would help to clarify whether the potters making Atticising vessels had access to local deposits or whether they had to procure the raw material from elsewhere, as it was suggested for Laconian-style black-figure production in Samos (Pipili 2018, p. 140).

## Pyrotechnology

All black gloss paint layers characterised in this work are compatible with the typical phase composition of Attic black gloss, which corresponds to a mixture of iron(II) oxides (hercynite and magnetite) and iron(III) oxides (hematite and maghemite). The presence of iron(II) oxides in all samples indicates that these black gloss specimens were fired under the typical three-stage oxidising-reducing-oxidising firing. However, the variability in the relative shape and size of the different iron-oxide peaks reveals small differences in crystallinity and composition between samples. This variability is directly connected to variations in the potters' control over the firing process, which is consistent with experimental firings of black gloss vessels (Balachandran 2019). The wood firing method induces localised variations of atmosphere in the firing chamber, which can affect the transformation of the iron oxides. This results in the observed mineralogical variability and the misfiring of some gloss layers.

Furthermore, some gloss diffractograms showed sharp hercynite peaks, suggesting well-crystallised hercynite and, therefore, a high oxygen fugacity during the reducing phase (Maggetti et al. 1981; Turnock and Eugster 1962). In comparison, low and broad hercynite peaks observed in other diffractograms, indicating poorly crystallised hercynite, can be attributed to a low oxygen fugacity during the reducing phase. This suggests variability in the intensity of reduction resulting from different gas compositions due to different fuel materials in combination with the degree of sealing of the kiln.

The observation of the gloss layer micrographs under BSE demonstrated that most specimens exhibit a vitrified gloss with bloating pores. This implies that the vessels were likely fired at max temperatures ranging from 850 to 950°C (Aloupi-Siotis 2020), which is consistent with the firing temperatures described in the literature (see the 'Previous studies of Attic gloss technology' section). Nevertheless, the

broken and flaky gloss layer of sample Pri602 could have been fired under 850°C (Aloupi-Siotis 2020), although the deterioration of this sample's gloss could also be due to post-depositional deterioration (Jones 2021, p. 94), or to a combination of the two factors above.

Overall, it can be safely assumed that both the Attic potters and the manufacturers of Atticising vessels followed a similar firing procedure concerning maximum temperature and kiln atmosphere. As a result, the Atticising black gloss was similarly vitrified and comparable to the quality of the Attic one. The variability observed demonstrates the difficulty for ancient potters to control the firing scheme and repeat it from one firing to the other. Therefore, the production of Atticising black gloss, despite its large scale, cannot be classified as production of a manufactory level, as is for instance the later Terra Sigillata.

## Connection between gloss mineralogy and surface appearance

To test previous suggestions correlating the external appearance of the black gloss with its mineralogical composition (Aloupi-Siotis 2008; Giorgetti et al. 2004; Gliozzo et al. 2004), a set of specimens corresponding to the most coherent fabric Ma-D were evaluated. The sherds from this fabric were selected because of their homogeneity from a ceramic body composition point of view, and it contains the highest number of samples with all surface appearances represented.

By comparing the diffractograms of the shiny, matt, and metallic gloss specimens of fabric Ma-D, it appears that the intensity and shape of the peaks correlate with the surface appearance of the gloss coatings (Fig. 8a). Shiny and metallic gloss specimens have similar intensities of both the hercynite and magnetite/maghemite main peaks, with the occurrence of hematite. Although showing similar diffraction patterns, shiny and metallic gloss specimens seem to be differentiated by the broadness of their peaks and, therefore, by a difference in the crystallinity of their iron oxide and spinel minerals. The matt gloss specimens, on the other hand, present high intensity of hercynite compared to the other iron oxides and spinels.

The same observations can be made with the Attic black gloss references from Iasos and Priene (Fig. 8b). The shiny and metallic gloss samples IA6 and IA11 present similar diffraction patterns as gloss samples M26 and M11 respectively. Furthermore, gloss Pri533, a matt gloss with a greenish hue, displays a high hercynite peak with almost no other identifiable iron oxide, which resembles what could be seen in matt gloss M17.

The variations seen in the size and shape of the peaks from samples of different surface appearances could reflect a correlation between mineralogy and surface finish. This



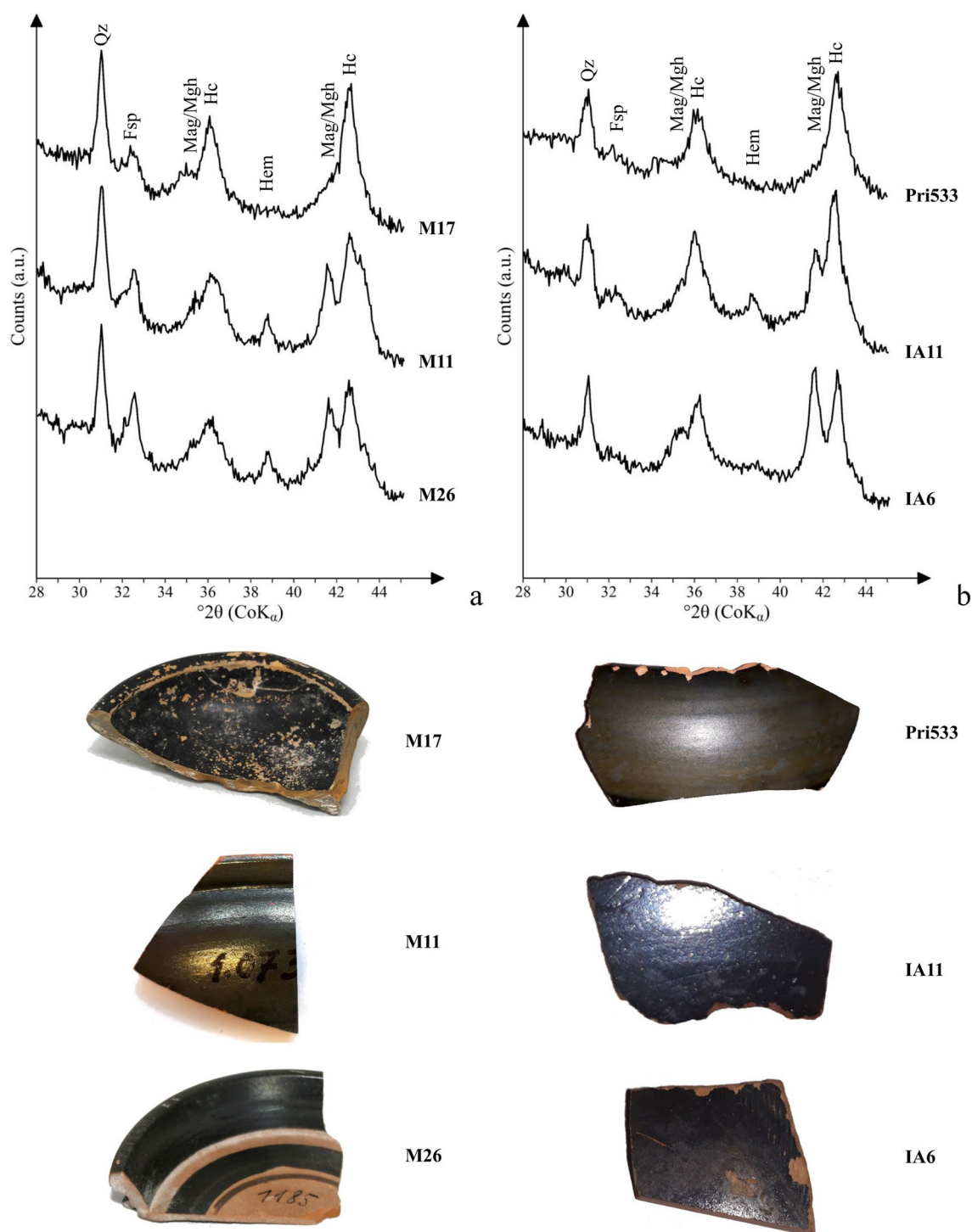


**Fig. 8** Diffraction patterns of the different surface appearance types observed and pictures of the respective samples. **a** Diffraction patterns of gloss specimens from fabric Ma-D. **b** Diffraction pattern of Attic gloss

specimens. M26 and IA6: Shiny; M11 and IA11: Metallic; M17: Matt; Pri533: Matt with greenish hue

appears to be consistent with previous observations suggesting that firing conditions influence the final appearance of black gloss (Giorgetti et al. 2004; Gliozzo et al. 2004). However, a more systematic investigation of a bigger sample

size would be needed to confirm these observations. Furthermore, it cannot be affirmed with certainty that those variations in surface appearance were intentionally produced or simply the result of the difficulty in firing condition control.

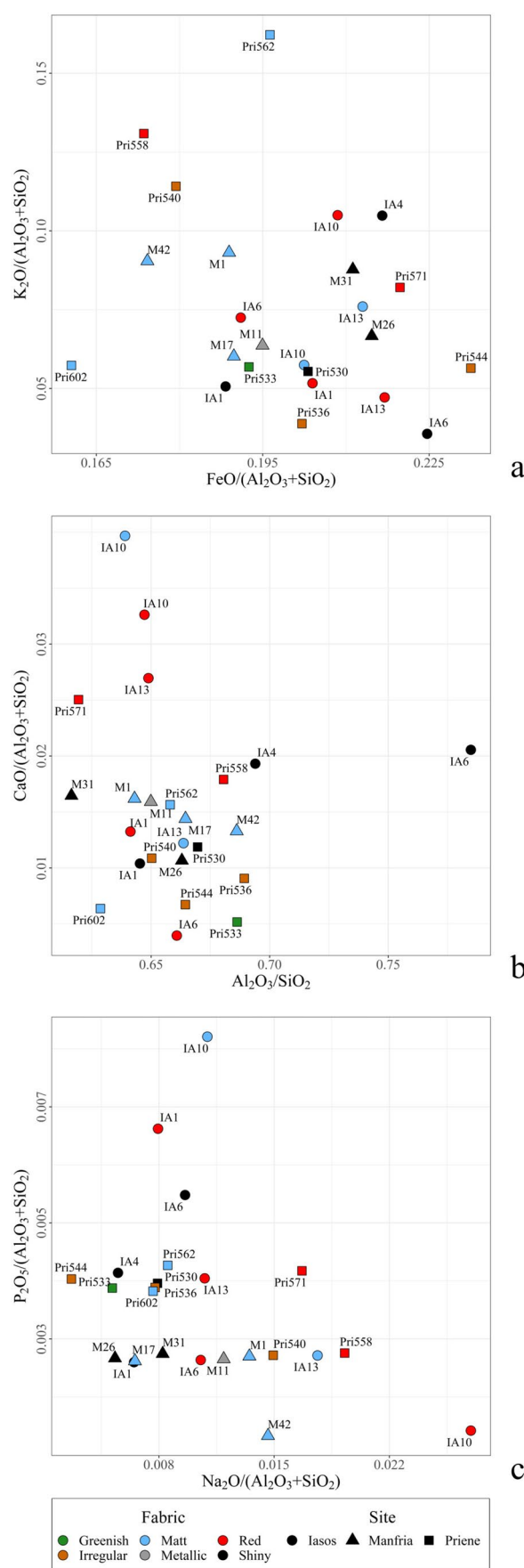
**Fig. 9** a–c Scatterplots based on the chemical characterisation of the samples from Iasos, Manfria, and Priene by SEM-EDS and labelled according to the visual appearance of their gloss

### Technological relationship between black and red gloss

The chemical characterisation of the red gloss samples showed rather low compositional differences between the red and the black layers, which is consistent with prior observations (Maish et al. 2006; Tite et al. 1982; Walton et al. 2009). Indeed, the clay paints for the manufacture of both gloss types have, in general, been prepared from non-calcareous, iron- and illite-rich clay, with a similar level of clay refinement.

Few variabilities could be observed in the calcite, soda, and potassium content of the red gloss specimens (Fig. 9). For instance, Pri558 is characterised by higher levels of potash in its gloss, compared to the other black and red gloss individuals. Pri571 on the other hand displays high calcite content in its paint layer, which could have affected the microstructure of the final gloss, resulting in the less compact structure observed in the BSE micrographs.

The four bichrome vessels from Iasos are especially interesting to discuss, as they have both black and red gloss decorations. The chemical composition of IA1 seems quite consistent between its two gloss colours. Similarly, the two gloss layers of IA13 display comparable chemical compositions, except for calcite (Fig. 9b). As already mentioned, this measurement should be regarded with caution, as the standard deviation of the CaO measurements for the red gloss of IA13 was rather high. The chemical composition of the black and red layers of sample IA6 mostly varies in terms of alumina to silica ratio (Fig. 9b), which could indicate different processing, and the use of a finer clay fraction for the manufacture of the black gloss layer. This difference in alumina and silica content, which are the main components of the clay paint, can affect the levels of the other measured elements by dilution, and therefore result in this apparent difference of composition between the IA6 black and red gloss layers. Finally, IA10 mainly shows variations of composition between its two colours in the phosphorus and soda levels (Fig. 9c). As discussed, the high  $P_2O_5$  content of IA10-black is probably due to measurement errors, as its standard deviation was rather high. The high concentration of sodium in the red layer might either reflect the addition of Na-rich materials during the manufacture of the clay paint or the result of post-depositional chemical modifications. The latter interpretation seems more likely, especially considering that red gloss layers are, in general, more porous than black layers because of their lower vitrification.



In general, the variations observed in the chemical content of the red gloss layers are still in the range of what was observed in the black layers (Figs. 5 and 7). Therefore, it can be assumed that these variabilities are only due to single artisanal variations rather than differences in the clay processing between black and red. On the contrary, this suggests that Attic potters and the manufacturers of Atticising vessels were using the same clay paint to produce either black or red gloss decorations.

The mineralogical composition of the Iasos red gloss ware indicated the presence of few hercynite and magnetite, whereas no such oxides were detected in the Priene red gloss ware (Fig. 5d). The difference between those vessels is that the Iasos samples are bichrome, bearing both black and red gloss decorations, while the Priene ones have only red gloss. As already suggested above, the mineralogical composition of the Priene red gloss indicates that these vessels were fired only in oxidising conditions, intending to produce only a red gloss. Contrarily, the red gloss layers on the bichrome vessels of Iasos were most probably fired in a single firing aimed at producing both black and red colours. One way to achieve that would be to stack the vessels in the kiln to have the intended red side be mostly protected from the reducing fumes, resulting in a red gloss, while the rest of the vessel would turn black (Aloupi-Siotis 2008; Amicone 2015). Another possibility would be the use of a coarser fraction of the same clay paint for the red gloss while the finest is used for the black gloss. Indeed, the coarser clay paint would not vitrify as the finer one would and, therefore, remained porous enough to turn back to red during the last oxidising phase of the firing, while the finer clay paint would remain black (Tite et al. 1982). It cannot be excluded that the bichrome vessels underwent multiple firings to produce the black gloss areas in a first firing, and the red gloss areas in a second, only oxidising firing (Aloupi-Siotis 2008; Richter 1951). Regardless of the employed technique, the presence of bichrome vessels shows the ingenuity of ancient potters and their control over and understanding of the firing process and conditions.

## Conclusions

Through an integrated archaeometric approach, this study demonstrates a direct technological similarity between the Attic and Atticising productions and shows that black gloss technology in the fourth century BCE is a rather homogeneous production technique. The few technological variabilities do not suggest strong differences in technological processes between production centres but, instead, point out that black gloss production was a traditional craft, which was not highly standardised and controlled, resulting in small

technological variations between workshops. Given the complexity of the production technique, black gloss vessels cannot be produced without prior technological know-how, strongly suggesting that the Atticising black gloss productions were not a simple imitation of the Attic black gloss technique. Instead, it shows that, by the fourth century BCE, potters making Atticising vases had the same technological knowledge as potters from Attica, suggesting a direct transmission of know-how through apprenticeship. This form of direct technological transmission implies the migration of experienced potters and vase painters from Attica towards the Greek colonies and other Mediterranean regions, possibly with the intention of starting a local business, thus teaching local potters in the process. Another possibility is that foreign apprentices based in Attica, or other regions where the technique was already applied, learned to produce black gloss and returned to their native land, where they utilised local materials and adapted to local stylistic influences, which eventually led to the development of an Atticising style. Such movements of Attic and Atticising vessel producers is, for instance, attested in the case of Atticising red-figure painters, who travelled within Magna Graecia in the Classical and Hellenistic periods (Denoyelle et al. 2018). Additionally, movements of Aegean potters towards Italy are already suggested to have taken place as early as the Late Bronze Age and resulted in a technological transmission and the local production of Mycenaean-styled black, brown, and red painted potteries in Italy (Jones et al. 2021). Similarly, the emigration of Attic potters is supported by a fourth century BCE decree recovered in Ephesus (ca. 25 km north of Priene), which states that the Ephesian *politeia* (citizenship) was offered to two Athenian potters, the brothers Kittios and Bakchios, on the condition that they produce ‘black potteries’ and the ‘hydria of the goddess’ (Gauthier 1985, pp. 150–151; Kratzmüller and Trinkl 2005).

**Supplementary Information** The online version contains supplementary material available at <https://doi.org/10.1007/s12520-023-01822-4>.

**Acknowledgements** This article is based on an M.Sc. thesis in Scientific Archaeology at the University of Tübingen by Baptiste Solard, presented in October 2021 under the supervision of Silvia Amicone, Christoph Berthold, and Christopher Miller. The authors would like to thank the Institute of Archaeology at the University College London, in particular Thomas Gregory and Patrick Quinn, for their help with the analyses of our materials and for giving us access to their laboratory equipment. In addition, for their help and feedback, the authors thank Beatrice Boese, Marcel Frenken, Sinem Haciosmanoğlu, Frieder Lauxmann, Madison McCartin, and Johannes Seidler. Finally, the authors would also like to acknowledge the Excellence Initiative (University of Tübingen), the Ministry for Science, Research, and Art of Baden-Württemberg, for their support during the preparation of this article. Constructive comments by anonymous reviewers and the editor helped us strengthen the paper and are much appreciated.

**Author contribution** Baptiste Solard: conceptualisation; methodology; formal analysis (ceramic petrography, SEM-EDS,  $\mu$ -XRD<sup>2</sup>);

investigation; writing—original and final draft; visualisation; project administration.

Silvia Amicone: conceptualisation, methodology, formal analysis (ceramic petrography), supervision of formal analysis (ceramic petrography, SEM-EDS), investigation, review and editing of original and final draft.

Eleni Aloupi-Siotis: conceptualisation, supervision of formal analysis (SEM-EDS), investigation, review and editing of final draft.

Lars Heinze: conceptualisation, formal analysis (p-XRF), investigation, review and editing of original and final draft, resources.

Fede Berti: investigation, review and editing of final draft, resources.

Claudia Lambrugo: investigation, review and editing of final draft, resources.

Christoph Berthold: methodology, supervision of formal analysis ( $\mu$ -XRD<sup>2</sup>), review and editing of final draft, resources, funding acquisition.

**Funding** Open Access funding enabled and organized by Projekt DEAL.

**Data availability** The authors confirm that the data supporting the findings of this study are available within the article and its supplementary materials.

The authors confirm that the data supporting the findings of this study (pXRF and SEM-EDS data) are available within the article and its supplementary materials. Additionally, the  $\mu$ -XRD<sup>2</sup> measurements and SEM-BSE micrographs supporting this study are openly available in an online data verse at <https://doi.org/10.7910/DVN/PMTQZJ>.

## Declarations

**Ethical approval** Not applicable.

**Competing interests** The authors declare no competing interests.

**Open Access** This article is licensed under a Creative Commons Attribution 4.0 International License, which permits use, sharing, adaptation, distribution and reproduction in any medium or format, as long as you give appropriate credit to the original author(s) and the source, provide a link to the Creative Commons licence, and indicate if changes were made. The images or other third party material in this article are included in the article's Creative Commons licence, unless indicated otherwise in a credit line to the material. If material is not included in the article's Creative Commons licence and your intended use is not permitted by statutory regulation or exceeds the permitted use, you will need to obtain permission directly from the copyright holder. To view a copy of this licence, visit <http://creativecommons.org/licenses/by/4.0/>.

## References

- Adamesteanu D (1958) Manfria (Gela). Scavo di una fattoria officina. *Notizie degli Scavi di Antichità* 12:290–334
- Aloupi-Siotis E (2008) Recovery and revival of attic vase-decoration techniques. What Can They Offer Archaeological Research? In: Lapatin K (ed) *Papers on special techniques in Athenian vases: Proceedings of a symposium held in connection with the exhibition "The colors of clay: special techniques in Athenian vases"*, at the Getty Villa, June 15–17, 2006. J. Paul Getty Museum, Los Angeles, pp 113–128

- Aloupi-Siotis E (2020) Ceramic technology: how to characterise black Fe-based glass-ceramic coatings. *Archaeol Anthropol Sci* 12:191. <https://doi.org/10.1007/s12520-020-01134-x>
- Amicone S (2015) Fourth-century BC black and red gloss pottery from Iasos: a technological approach. In: Gürtekin-Demir RG, Cevizoglu H, Polat Y, Polat G (eds) *Keramos. Ceramics: A Cultural Approach: Proceedings of the First International Conference at Ege University (May 9–13, 2001, Izmir)*. Bilgin Kültür Sanat Yayınları, Ankara, pp 25–39
- Amicone S (2016) Rediscovering the fattoria officina of Manfria (Gela): towards a new chronological and functional interpretation of the site. *Acordia Res Paper* 14:123–154
- Amicone S, Müller NS, Heinze L, Schneider G, Neumann S, Fenn N, Kiriati E (2023) Four centuries of cooking wares at Priene: tracing transformation in supply and trade patterns in Western Asia Minor (Turkey). *Advances in Archaeomaterials*
- Amicone S, Fenn N, Heinze L, Schneider G (2014) Cooking pottery in Priene. Imports and Local/Regional Production from Late Classical to Late Hellenistic Times. *Frankfurter elektronische Rundschau zur Altertumskunde* 25:1–27
- Avila A, Queralt-Mitjans I, Alarcón M (1997) Mineralogical composition of African dust delivered by red rains over northeastern Spain. *J Geophys Res: Atmos* 102:21977–21996. <https://doi.org/10.1029/97JD00485>
- Balachandran S (2019) Bringing back the (ancient) bodies: the Potters' sensory experiences and the firing of red, black and purple Greek vases. *Arts* 8:70–93. <https://doi.org/10.3390/arts8020070>
- Barbera G, Barone G, Mazzoleni P (2018) Excursus sulle caratteristiche composizionali dei sedimenti argillosi della Sicilia centro-meridionale. In: Ingoglia C (ed) *Risorse ambientali e impianti produttivi a Gela: Risultati di una ricerca congiunta tra le Università di Messina e Catania*. Edipuglia, Bari, pp 35–38
- Barone G, Mazzoleni P, Raneri S, Spagnolo G, Santostefano A (2017) Coroplastic art in Sicily: an investigation on provenance and manufacturing technology of Greek architectural terracottas from Gela (Italy). *Mediterr Archaeol Archaeom* 17:89–101. <https://doi.org/10.5281/zenodo.258087>
- Barone G, Mazzoleni P, Spagnolo G, Aquila E (2012) The transport amphorae of Gela: a multidisciplinary study on provenance and technological aspects. *J Archaeol Sci* 39:11–22. <https://doi.org/10.1016/j.jas.2011.06.018>
- Bente K, Sobott R, Berthold C (2013) Phase analytical and microstructural study of black glosses on Attic red-figure vases by XRD (GADDS), Mössbauer spectroscopy, and TEM. In: Ramming B, Stilborg O, Helfert M (eds) *Naturwissenschaftliche Analysen vor- und frühgeschichtlicher Keramik III: Methoden, Anwendungsbereiche, Auswertungsmöglichkeiten*. Verlag Dr. Rudolf Habelt, Bonn
- Berthold C, Bjeoumikhov A, Brügemann L (2009) Fast XRD<sup>2</sup> microdiffraction with focusing X-ray microlenses. *Part Part Syst Charact* 26:107–111. <https://doi.org/10.1002/ppsc.200800038>
- Berthold C, Mentzer S (2017) Microdiffraction. In: Nicosia C, Stoops G (eds) *Archaeological Soil and Sediment Micromorphology*. John Wiley & Sons, pp 417–427
- Berthold C, Zimmer KB, Scharf O, Koch-Brinkmann U, Bente K (2017) Nondestructive, optical and X-ray analytics with high local resolution on Attic white-ground lekythoi. *J Archaeol Sci Rep* 16:513–520. <https://doi.org/10.1016/j.jasrep.2016.02.008>
- Berti F (2013) La ceramica attica a vernice nera di Iasos nel V e IV secolo a.C. In: Brun P, Cavalier L, Konuk K, Prost F (eds) *Euploia. La Lycie et la Carie antiques : Dynamiques des territoires, échanges et identités - Actes du colloque de Bordeaux, 5, 6 et 7 novembre 2009*. Ausonius, Bordeaux, pp 233–240
- Bimson M (1956) The technique of Greek Black and Terra Sigillata Red. *Ant J* 36:200–204. <https://doi.org/10.1017/S0003581500061096>



- 1209 Binns CF, Fraser AD (1929) The genesis of the Greek Black Glaze. *Am J Archaeol* 33:1–9
- 1210 Boardman J (1974) Athenian black figure vases: a handbook. Thames & Hudson, London
- 1211 Chaviara A (2014) A technical approach to Attic-pottery production during the historic period: raw materials and the black glaze. In: Kassianidou V, Dikomitou-Eliadou M (eds) The NARNIA Project: Integrating approaches to ancient material studies. University of Cyprus, Nicosia, NARNIA Project and the Archaeological Research Unit, pp 54–67
- 1212 Chaviara A, Aloupi-Siotis E (2016) The story of a soil that became a glaze: chemical and microscopic fingerprints on the Attic vases. *J Archaeol Sci Rep* 7:510–518. <https://doi.org/10.1016/j.jasrep.2015.08.016>
- 1223 Cianchetta I, Trentelman K, Maish J, Saunders D, Foran B, Walton MS, Sciau P, Wang T, Pouyet E, Cotte M, Meirer F, Liu Y, Pianetta P, Mehta A (2015) Evidence for an unorthodox firing sequence employed by the Berlin Painter: deciphering ancient ceramic firing conditions through high-resolution material characterization and replication. *J Anal Atom Spectrom* 30:666–676. <https://doi.org/10.1039/c4ja00376d>
- 1224 Cianchetta I, Trentelman K, Walton MS, Maish J, Mehta A, Foran B (2016) Reverse engineering ancient Greek ceramics: morphological and spectral characterization of replicates. *J Am Ceram Soc* 99:1792–1801. <https://doi.org/10.1111/jace.14123>
- 1231 Cohen B (2006) Coral-red gloss: painters, and painter-potters. In: Cohen B (ed) The colors of clay: Special techniques in Athenian vases. J. Paul Getty Museum, Los Angeles, pp 44–70
- 1232 Cook JM (1965) Old Smyrna: fourth-century black glaze. *Annu Br Sch Athens* 60:143–153. <https://doi.org/10.1017/S0068245400013903>
- 1233 Denoyelle M, Pouzadoux C, Silvestrelli F (eds) (2018) Mobilità dei pittori e identità delle produzioni: Ricerche sulla ceramica italiana 1. Cahiers du Centre Jean Bérard, vol 25. Publications du Centre Jean Bérard, Naples
- 1243 Farnsworth M, Wisely H (1958) Fifth century intentional red glaze. *Am J Archaeol* 62:165–173
- 1245 Gauthier P (1985) Les cités grecques et leur bienfaiteurs (IVe-Ier siècle avant J.-C.) : Contribution à l'histoire des institutions. Bulletin de correspondance hellénique, Supplément, XII. A. Bontemps, Limoges
- 1249 Giorgetti G, Gliozzo E, Memmi I (2004) Tuscan black glosses : a mineralogical characterization by high resolution techniques. *Eur J Mineral* 16:493–503. <https://doi.org/10.1127/0935-1221/2004/0016-0493>
- 1253 Gliozzo E, Kirkman IW, Pantos E, Memmi Turbanti I (2004) Black gloss pottery: production sites and technology in Northern Etruria, Part II: Gloss Technology. *Archaeometry* 46:227–246. <https://doi.org/10.1111/j.1475-4754.2004.00154.x>
- 1257 Gliozzo E, Memmi Turbanti I (2004) Black gloss pottery: production sites and technology in Northern Etruria, Part I: Provenance Studies. *Archaeometry* 46:201–225. <https://doi.org/10.1111/j.1475-4754.2004.00153.x>
- 1261 Heinze L (2014) Attic imports and their influence on the production of local fine-ware in Late Classical and Early Hellenistic Priene. In: Kotsou E, Kazakou M, Giannoulaki P (eds) Η Έπιστημονική Συναντησιγία Την Ελληνιστική Κεραμική. Ταμείο Αρχαιολογικών Πορών και Απαλλοτριώσεω, Athens, pp 313–318
- 1267 Heinze L (2023) Untersuchungen zur spätklassischen und frühhellenistischen Keramik von Priene. Priene, vol 6. Reichert, Wiesbaden
- 1269 Helfert M (2013) Die portable energiedispersive Röntgenfluoreszenzanalyse (P-ED-RFA) – Studie zu methodischen und analytischen Grundlagen ihrer Anwendung in der archäologischen Keramikforschung. In: Ramminger B, Stilborg O, Helfert M (eds) Naturwissenschaftliche Analysen vor- und frühgeschichtlicher Keramik III: Methoden, Anwendungsbereiche, Auswertungsmöglichkeiten. Verlag Dr. Rudolf Habelt, Bonn, pp 15–47
- 1275 Helfert M, Mecking O, Lang F, von Kaenel H-M (2011) Neue Perspektiven für die Keramikanalytik. Zur Evaluation der portablen energiedispersiven Röntgenfluoreszenzanalyse (P-ED-RFA) als neues Verfahren für die geochemische Analyse von Keramik in der Archäologie. Frankfurter elektronische Rundschau zur Altertumskunde 14:1–30
- 1281 Hofmann U (1962) The chemical basis of ancient Greek vase painting. *Angew Chem Int Ed* 1:341–350. <https://doi.org/10.1002/anie.196203411>
- 1284 Ingoglia C, Barone G, Mazzoleni P, Aquilia E (2018) Ceramica fine e archeometria: la produzione locale a Gela. In: Ingoglia C (ed) Risorse ambientali e impianti produttivi a Gela: Risultati di una ricerca congiunta tra le Università di Messina e Catania. Edipuglia, Bari, pp 57–69
- 1289 Jones RE (2021) The decoration and firing of ancient Greek pottery: a review of recent investigations. *Adv Archaeomat* 2:67–127. <https://doi.org/10.1016/j.aia.2021.07.002>
- 1292 Jones RE, Levi ST, Bettelli M, Cannavò V (2021) Italo-Mycenaean and other Aegean-influenced pottery in Late Bronze Age Italy: the case for regional production. *Archaeol Anthropol Sci* 13:23. <https://doi.org/10.1007/s12520-020-01245-5>
- 1296 Kingery D (1991) Attic pottery gloss technology. *Archaeomaterials* 5:47–54
- 1298 Konak N, Şenel M (2002) Geological map of Turkey in 1/500.000 scale: Denizli sheet. General Directorate of Mineral Research and Exploration, Ankara
- 1301 Kratzmüller B, Trinkl E (2005) Von Athleten und Töpfern - ephesischen Bürgern auf der Spur. In: Brandt B, Verena G, Sabine L (eds) Synergia. Phoibos, Wien, pp 157–167
- 1304 Lambrugo C, Heinze L, Amicone S (2019) Back to Manfredia farm: continuity or disruption in the countryside of Gela in the 4<sup>th</sup> century BC. In: Perego E, Scopacasa R, Amicone S (eds) Collapse or survival: Micro-dynamics of crisis and endurance in the ancient central Mediterranean. Oxbow Books, Oxford, pp 57–80
- 1309 Lühl L, Hesse B, Mantouvalou I, Wilke M, Mahlkow S, Aloupi-Siotis E, Kanngiesser B (2014) Confocal XANES and the Attic black glaze: the three-stage firing process through modern reproduction. *Analy Chem* 86:6924–6930. <https://doi.org/10.1021/ac500990k>
- 1313 Madrid i Fernández M, Sinner AG (2019) Analysing technical choices: improving the archaeological classification of Late Republican Black Gloss pottery in north-eastern Hispania consumption centres. *Archaeol Anthropol Sci* 11:3155–3186. <https://doi.org/10.1007/s12520-018-0748-x>
- 1318 Maggetti M, Galetti G, Schwander H, Picon M, Wessicken R (1981) Campanian pottery; the nature of the black coating. *Archaeometry* 23:199–207
- 1319 Maish J, Svoboda M, Lansing-Maish S (2006) Technical studies of some attic vases in the J. Paul Getty Museum. In: Cohen B (ed) The colors of clay: Special techniques in Athenian vases. J. Paul Getty Museum, Los Angeles, pp 8–16
- 1325 Maniatis Y, Aloupi E, Stalios AD (1993) New evidence for the nature of the Attic black gloss. *Archaeometry* 35:23–34. <https://doi.org/10.1111/j.1475-4754.1993.tb01021.x>
- 1327 Maniatis Y, Simopoulos A, Kostikas A, Perdikatsis V (1983) Effect of reducing atmosphere on minerals and iron oxides developed in fired clays: the role of Ca. *J Am Cer Soc* 66:773–781. <https://doi.org/10.1111/j.1151-2916.1983.tb10561.x>
- 1332 Mirti P, Casoli A, Calzetti L (1996) Technology of production of fine pottery excavated on a Western Greek site investigated by scanning electron microscopy coupled with energy-dispersive X-ray detection. *X-Ray Spectrometry* 25:103–109. [https://doi.org/10.1002/\(SICI\)1097-4539\(199605\)25:3<103::AID-XRS151%3e3.0.CO;2-V](https://doi.org/10.1002/(SICI)1097-4539(199605)25:3<103::AID-XRS151%3e3.0.CO;2-V)

- Montana G, Cau Ontiveros MÁ, Polito AM, Azzaro E (2011) Characterisation of clayey raw materials for ceramic manufacture in ancient Sicily. *Appl Clay Sci* 53:476–488. <https://doi.org/10.1016/j.clay.2010.09.005>
- Muhs DR, Budahn J, Avila A, Skipp G, Freeman J, Patterson D (2010) The role of African dust in the formation of Quaternary soils on Mallorca, Spain and implications for the genesis of Red Mediterranean soils. *Quat Sci Rev* 29:2518–2543. <https://doi.org/10.1016/j.quascirev.2010.04.013>
- Muşkara Ü, Kalaycı K (2021) The feasibility of PXRF for discriminating Attic Black-figure painters using pigment analysis. *Mediterr Archaeol Archaeom* 21:237–255. <https://doi.org/10.5281/zenodo.4574639>
- Noble JV (1960) The technique of attic vase-painting. *Am J Archaeol* 64:307–318. <https://doi.org/10.2307/501329>
- Noll W, Holm R, Born L (1975) Painting of ancient ceramics. *Angew Chem Int Ed Engl* 14:602–613. <https://doi.org/10.1002/anie.197506021>
- Pipili M (2018) Laconian pottery. In: Powell A (ed) *A Companion to Sparta*. John Wiley & Sons, Hoboken, pp 124–153
- Quinn PS (2013) Ceramic petrography: the interpretation of archaeological pottery & related artefacts in thin section. Archaeopress, Oxford
- Quinn PS (2022) Thin section petrography, geochemistry & scanning electron microscopy of archaeological ceramics. archaeopress, Oxford
- Raack W (2020) Priene in Antike und Mittelalter - eine Ergebnisskizze der Arbeiten seit 1998. In: Raack W, Filges A, Mert JH (eds) *Priene von der Spätklassik bis zum Mittelalter: Ergebnisse und Perspektiven der Forschungen seit 1998*. Habelt-Verlag, Bonn, pp 1–34
- Richter GMA (1951) Accidental and intentional red glaze on Athenian vases. *Ann Brit School Athens* 46:143–150. <https://doi.org/10.1017/S0068245400018414>
- Rodriguez-Navarro C, Di Lorenzo F, Elert K (2018) Mineralogy and physicochemical features of Saharan dust wet deposited in the Iberian Peninsula during an extreme red rain event. *Atmos Chem Phys* 18:10089–10122. <https://doi.org/10.5194/acp-18-10089-2018>
- Rumscheid F (1998) *Priene: Führer durch das "Pompeji Kleinasien"*. Ege Yayinlari, Istanbul
- Santostefano A, Spagnolo G, Barone G, Mazzoleni P (2018) La produzione di coroplastica e di terrecotte architettoniche a Gela in Età Arcaica e Classica. In: Ingoglia C (ed) *Risorse ambientali e impianti produttivi a Gela: Risultati di una ricerca congiunta tra le Università di Messina e Catania*. Edipuglia, Bari, pp 77–84
- Scarpelli R, Clark RJH, de Francesco AM (2014) Archaeometric study of black-coated pottery from Pompeii by different analytical techniques. *Spectrochimica acta Part A, Mol Biomolecular Spectroscopy* 120:60–66. <https://doi.org/10.1016/j.saa.2013.09.139>
- Spagnolo G, Barone G, Mazzoleni P, Aquilia E (2018) Le anfore da trasporto e la ceramica medio-grossolana di Gela in Età Greca: caratterizzazione e tecniche produttive. In: Ingoglia C (ed) *Risorse ambientali e impianti produttivi a Gela: Risultati di una ricerca congiunta tra le Università di Messina e Catania*. Edipuglia, Bari, pp 43–56
- Tang CC, MacLean EJ, Roberts MA, Clarke DT, Pantos E, Prag AJNW (2001) The study of Attic black gloss sherds using synchrotron X-ray diffraction. *J Archaeol Sci* 28:1015–1024. <https://doi.org/10.1006/jasc.2000.0608>
- Tite MS, Bimson M, Freestone IC (1982) An examination of the high gloss surface finishes on Greek Attic and Roman Samian Wares. *Archaeometry* 24:117–126. <https://doi.org/10.1111/j.1475-4754.1982.tb00994.x>
- Turnock AC, Eugster HP (1962) Fe–Al oxides: phase relationships below 1,000 C. *J Petrol* 3:533–565. <https://doi.org/10.1093/petrology/3.3.533>
- Vaag LE, Nørskov V, Lund J (2002) The Maussolleion at Halikarnassos. The pottery. Ceramic Material and Other Finds from Selected Contexts. Reports of the Danish Archaeological Expeditions to Bodrum, vol 7. Jutland Archaeological Society, Copenhagen
- Vendrell-Saz M, Pradell T, Molera J, Aliaga S (1991) Proto-Campanian and A-Campanian ceramics: characterization of the differences between the black coatings. *Archaeometry* 33:109–117. <https://doi.org/10.1111/j.1475-4754.1991.tb00689.x>
- Walton MS, Doehne E, Trentelman K, Chiari G, Maish J, Buxbaum A (2009) Characterization of coral red slips on Greek Attic pottery. *Archaeometry* 51:383–396. <https://doi.org/10.1111/j.1475-4754.2008.00413.x>
- Walton MS, Trentelman K, Cianchetta I, Maish J, Saunders D, Foran B, Mehta A (2014) Zn in Athenian black gloss ceramic slips: a trace element marker for fabrication technology. *J Am Ceram Soc* 98:430–436. <https://doi.org/10.1111/jace.13337>
- Winter A (1978) *Die antike Glanztonkeramik: Praktische Versuche*. Keramikforschungen, vol 3. Philipp von Zabern, Mainz am Rhein
- Yaalon DH (1997) Soils in the Mediterranean region: what makes them different? *Catena* 28:157–169. [https://doi.org/10.1016/S0341-8162\(96\)00035-5](https://doi.org/10.1016/S0341-8162(96)00035-5)

**Publisher's note** Springer Nature remains neutral with regard to jurisdictional claims in published maps and institutional affiliations.



|          |              |
|----------|--------------|
| Journal: | <b>12520</b> |
| Article: | <b>1822</b>  |

## Author Query Form

**Please ensure you fill out your response to the queries raised below and return this form along with your corrections**

Dear Author

During the process of typesetting your article, the following queries have arisen. Please check your typeset proof carefully against the queries listed below and mark the necessary changes either directly on the proof/online grid or in the 'Author's response' area provided below

| Query               | Details Required   | Author's Response |
|---------------------|--|-------------------|
| <a href="#">AQ1</a> | Please check if the author names and affiliations are captured and presented correctly.  |                   |
| <a href="#">AQ2</a> | Please check if the section headings are assigned to appropriate levels.   |                   |
| <a href="#">AQ3</a> | Please check Supplementary material citations if captured and presented correctly.   |                   |
| <a href="#">AQ4</a> | Please check if the tables and their corresponding table footnotes are presented correctly; otherwise, kindly amend as deemed necessary. |                   |
| <a href="#">AQ5</a> | References 'Amicone et al. (2023)' are given in list but not cited in text. Please cite in text or delete them from list.                |                   |